Lawrence Berkeley Laboratory
UNIVERSITY OF CALIFORNIA

ENERGY & ENVIRONMENT DIVISION

To be published as a chapter in COMPREHENSIVE TREATISE ON ELECTROCHEMISTRY, Volume VII, Eds. J.O'M. Bockris, B.E. Conway, E.B. Yeager, New York: Plenum Publishing Corp. (in press)

RECHARGEABLE HIGH-TEMPERATURE BATTERIES

Elton J. Cairns

January 1981

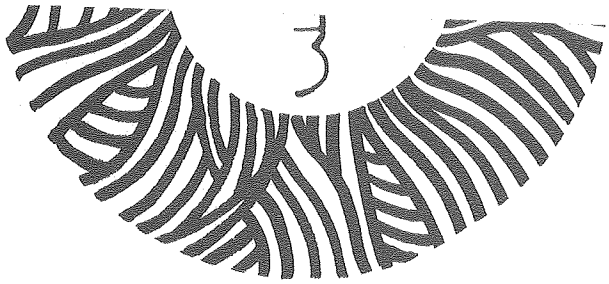

Prepared for the U.S. Department of Energy under Contract W-7405-ENG-48

DISCLAIMER

RECHARGEABLE HIGH-TEMPERATURE BATTERIES

Elton J. Cairns
Associate Laboratory Director
Head, Energy and Environment Division
Lawrence Berkeley Laboratory
University of California
Berkeley, California 94720

in

COMPREHENSIVE TREATISE ON ELECTROCHEMISTRY, VOLUME VII

J.O'M. Bockris, B.E. Conway, E.B. Yeager, eds.

Plenum Publishing Corporation
New York, NY

(in press)

1. INTRODUCTION

Since the mid-1960's there has been a growing research and development effort in the area of high specific energy, high specific power rechargeable batteries for use in electric vehicles, electric utility networks, and solar- and wind-powered electric generator systems. For a variety of reasons, including scientific, technological, and economic, high-temperature, non-aqueous systems have been found to be the most attractive candidates for the above relatively large-scale applications. Only the high-temperature cells offer the attractive combination of features sought for the cited applications: a specific energy above 100 W-h/kg, a specific power above 100 W/kg, a cycle life in excess of 500 cycles (at 100% depth of discharge), and a projected cost of less than $50* per kWh of energy storage capability.

Some perspective regarding the relative specific energies of various electrochemical cells can be gained by studying Figure 1, which shows the theoretical specific energy of various cells, plotted against the equivalent weights of the reactants (or products). The theoretical specific energy is defined as the Gibbs free energy change for the overall cell reaction, divided by the corresponding weights of the reactants.

$$\text{Theoretical Specific Energy} = \frac{-\Delta G}{\Sigma \nu_i M_i} \qquad (1)$$

where ν_i is the number of moles of reactant i

M_i is the molecular weight of reactant i

It is evident from Figure 1 that the higher theoretical specific energy values correspond to cells with low-equivalent-weight reactants, and with large electronegativity differences between the reactants. The alkali metals are very attractive reactants for the negative electrodes, and the chalcogens and

---

*1979 dollars

FIGURE 1

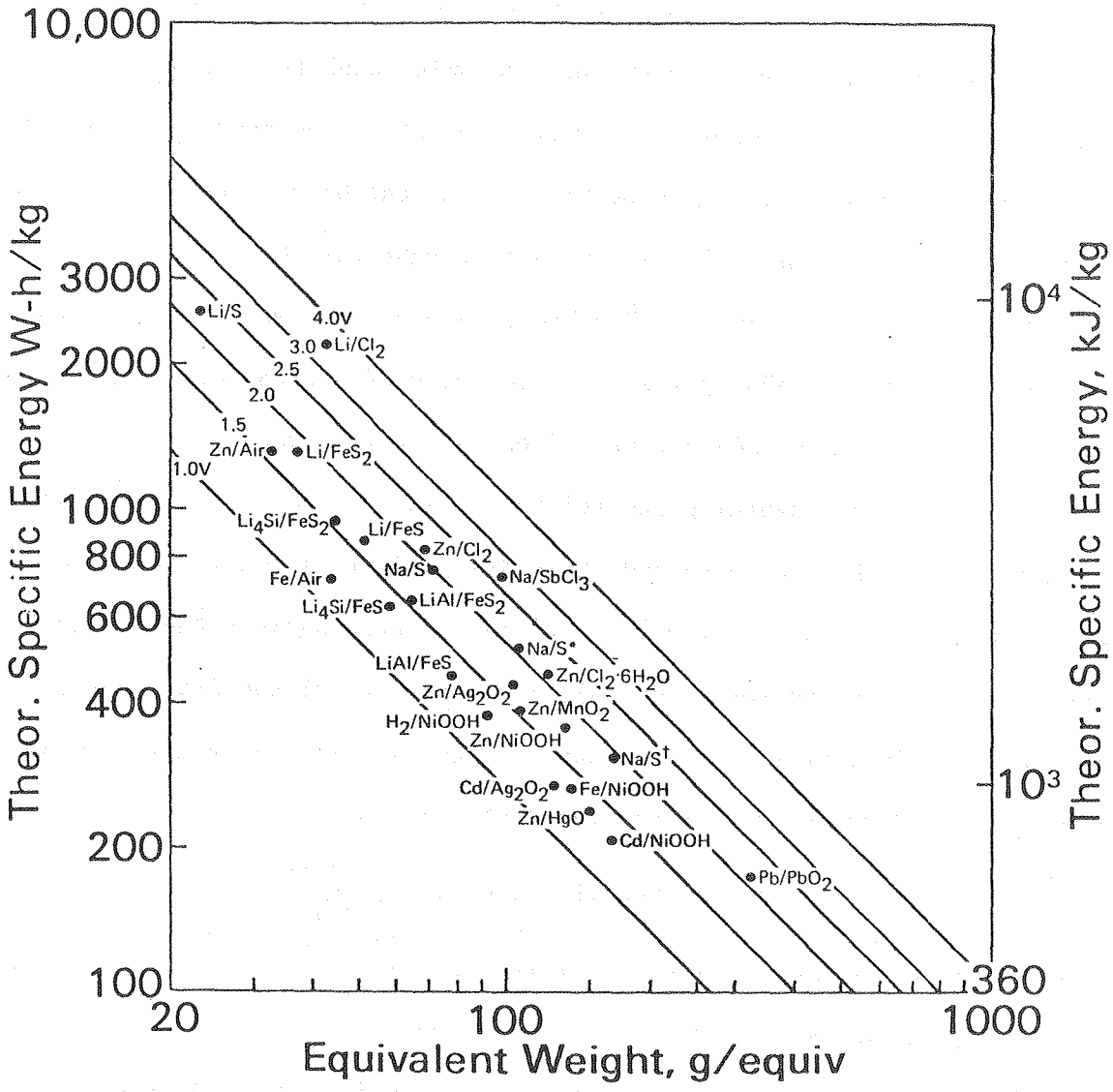

XBL 7912-13725

halogens (and some compounds containing them) are very attractive reactants for the positive electrodes. Notice that most of the high-specific-energy couples involve reactants that are incompatible with aqueous electrolytes. Among the non-aqueous electrolytes, only those that are used at elevated temperatures have high conductivities ($>0.1\Omega^{-1}cm^{-1}$), consistent with specific power values above 100 W/kg. A summary of other desirable characteristics for cell reactants and electrolytes is given in Table 1.[1]

The electrolytes which are most useful in high-temperature cells are solid ionic conductors (either ceramics or glasses) or molten salts. These electrolytes must be chemically stable in contact with both the negative and positive electrode reactants, and must have a decomposition potential safely above the maximum operating voltage of the cell (unless a component of the electrolyte is a cell reaction product). The above considerations significantly narrow the field of choices, so that high-temperature cells with sodium electrodes now must use solid electrolytes (because sodium is soluble in its molten halides, yielding an electronically conductive electrolyte), and cells with lithium (and some other) electrodes now must use molten salt electrolytes (because there are no solid lithium ion conductors sufficiently stable to lithium). Therefore, there is a natural grouping of high-temperature cells which will be followed in the discussion below: sodium cells with solid electrolytes, and lithium (and calcium) cells with molten-salt electrolytes.

2. CELLS WITH SOLID ELECTROLYTES

All of the high-temperature cells with solid electrolytes under current development contain molten sodium as the negative electrode, and rely upon sodium ion conduction in the electrolyte. The positive electrodes for these cells may be sulfur, a sulfide, or a halide. These cells operate at temperatures in the range 200-400°C.

TABLE 1

DESIRABLE CHARACTERISTICS OF SYSTEMS FOR HIGH-PERFORMANCE ELECTROCHEMICAL CELLS

Characteristic	Anode reactant	Cathode reactant	Electrolyte
Electronegativity	Low ($\sim$1)	High (>1.5)	--
Equivalent weight (g/g-equiv.)	Low (<30)	Low (<30)	Low* (<30)
Conductivity (ohm^{-1} cm^{-1})	High (>10^{4})	High (>10^{4})	High (>1)
Electrochemical reaction rate (i_o, A/cm^2)	High (>10^{-3})	High (>10^{-3})	High (>10^{-3})
Solubility in electrolyte (mol %)	Low (<0.1)	Low (<0.1)	--
Mass transport rate (equiv/ $sec-cm^2$)	High (>10^{-4})	High (>10^{-4})	High (>10^{-4})

*A more important criterion for the electrolyte is low density.

2.1. The Sodium/Beta-Alumina/Sulfur Cell

The heart of the Na/β-Al_2O_3/S cell is the ceramic electrolyte, called beta alumina.[2] Actually, the electrolyte is a sodium aluminate of the composition $Na_2O \cdot 11Al_2O_3$, consisting of hexagonal layers of spinel-like blocks containing aluminum and oxygen atoms, the layers being spaced apart by aluminum-oxygen bridges. The sodium ions are located in planes perpendicular to the C axis of the crystals, and are mobile in these planes. The conductivity is about $0.3\Omega^{-1}cm^{-1}$ at 300°C for single-crystal β-Al_2O_3, and 5 to 20 times lower for polycrystalline material. A related form of this material, β''-Al_2O_3, with a greater C axis spacing, has a higher conductivity of $0.3\Omega^{-1}cm^{-1}$ for the polycrystalline form at 300°C. A typical composition for $\beta''Al_2O_3$ is $Na_2O \cdot 6Al_2O_3$ with up to 2 w/o MgO and/or Li_2O to stabilize the structure.

The beta-alumina electrolyte for Na/S cells is prepared (usually by pressing and sintering) in a tubular form, with a wall thickness of 1-2 mm. The original form of the cell, reported by Kummer and Weber,[3] is shown schematically in Figure 2, with sodium inside the electrolyte tube, and sulfur outside. The molten sodium, being an excellent electronic conductor, acts as its own current collector, and makes contact with the sodium container, which serves as the negative terminal of the cell. The sulfur and the polysulfides which form during discharge are poor electronic conductors, so a current collector network of graphite fibers (e.g., in the form of a felt matting) is used in the sulfur electrode, providing an electronically conductive pathway from the positive terminal through the metal cell case, to the sites of electrochemical reaction near or at the surface of the electrolyte.

The overall cell reaction is the conversion of sodium and sulfur to sodium sulfides at about 350°C:

FIGURE 2

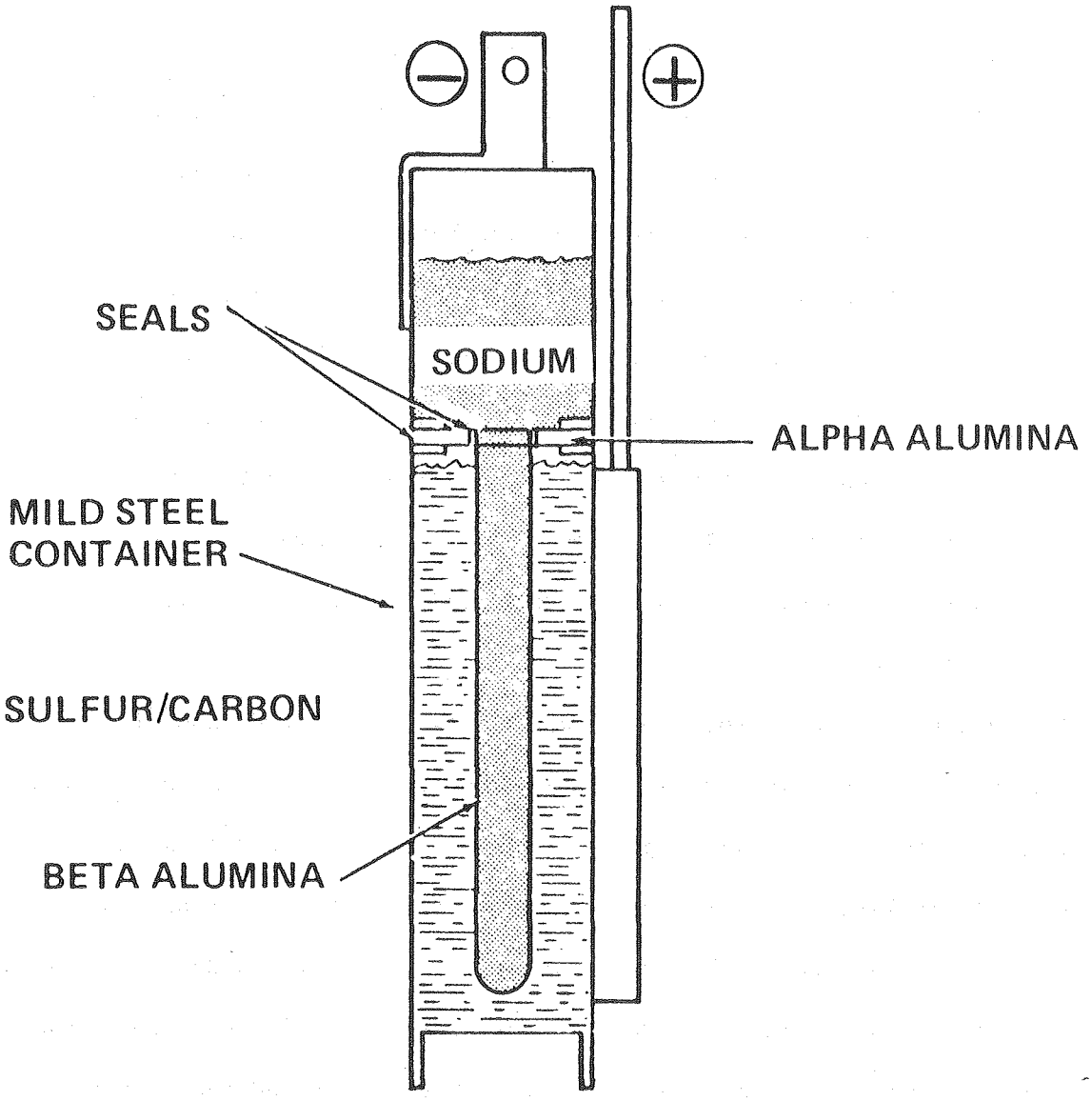

XBL 802-8067

$$2Na + xS \rightarrow Na_2S_x \quad (2)$$

The phase diagram showing the coexistence of two immiscible sulfur-rich liquid phases is presented in Figure 3.[4] Starting with the cell in the fully charged state at 350° C, the positive electrode is essentially pure liquid sulfur, with a potential of 2.1-2.2 V vs. the Na electrode. As the cell is discharged, a sodium polysulfide is formed according to Equation 2. When the amount of polysulfide formed exceeds the solubility limit in sulfur (a fraction of a percent), a separate polysulfide phase forms, having a composition (at 350° C) of $Na_2S_{5.2}$, comprised largely of Na_2S_5 and Na_2S_6. This phase has a high electrolytic conductivity. The amount of polysulfide phase increases at the expense of the sulfur phase as discharge continues. The reversible cell potential remains 2.07-2.08 V so long as the two phases coexist (see Figure 4).

When all of the sulfur is converted into polysulfide, the overall composition of the positive electrode is $Na_2S_{5.2}$. Further discharge is proposed by Ludwig[5] to take place as follows:

$$^{-}S_3 - S_2^{-} + e^{-} \rightarrow {}^{-}S_3 \cdots S_2^{=} \quad (3)$$

$$^{-}S_3 \cdots S_2^{=} + e^{-} \rightarrow S_3^{=} + S_2^{=} \quad (4)$$

$$2S_3^{=} \rightarrow S_2^{=} + S_4^{=} \quad (5)$$

$$S_2^{=} + 2S_5^{=} \rightarrow 3S_4^{=} \quad (6)$$

Reactions 3 and 4 are electrochemical, and are followed by chemical reactions 5 and 6, resulting in the conversion of the polysulfide phase to the overall composition Na_2S_4 (comprised of a mixture of Na_2S_2, Na_2S_4, and Na_2S_5). As discharge continues, a similar mechanism operates on Na_2S_4:

$$^{-}S_2 - S_2^{-} + e^{-} \rightarrow {}^{=}S_2 \cdots S_2^{-} \quad (7)$$

$$^{=}S_2 \cdots S_2^{-} + e^{-} \rightarrow 2S_2^{=} \quad (8)$$

FIGURE 3

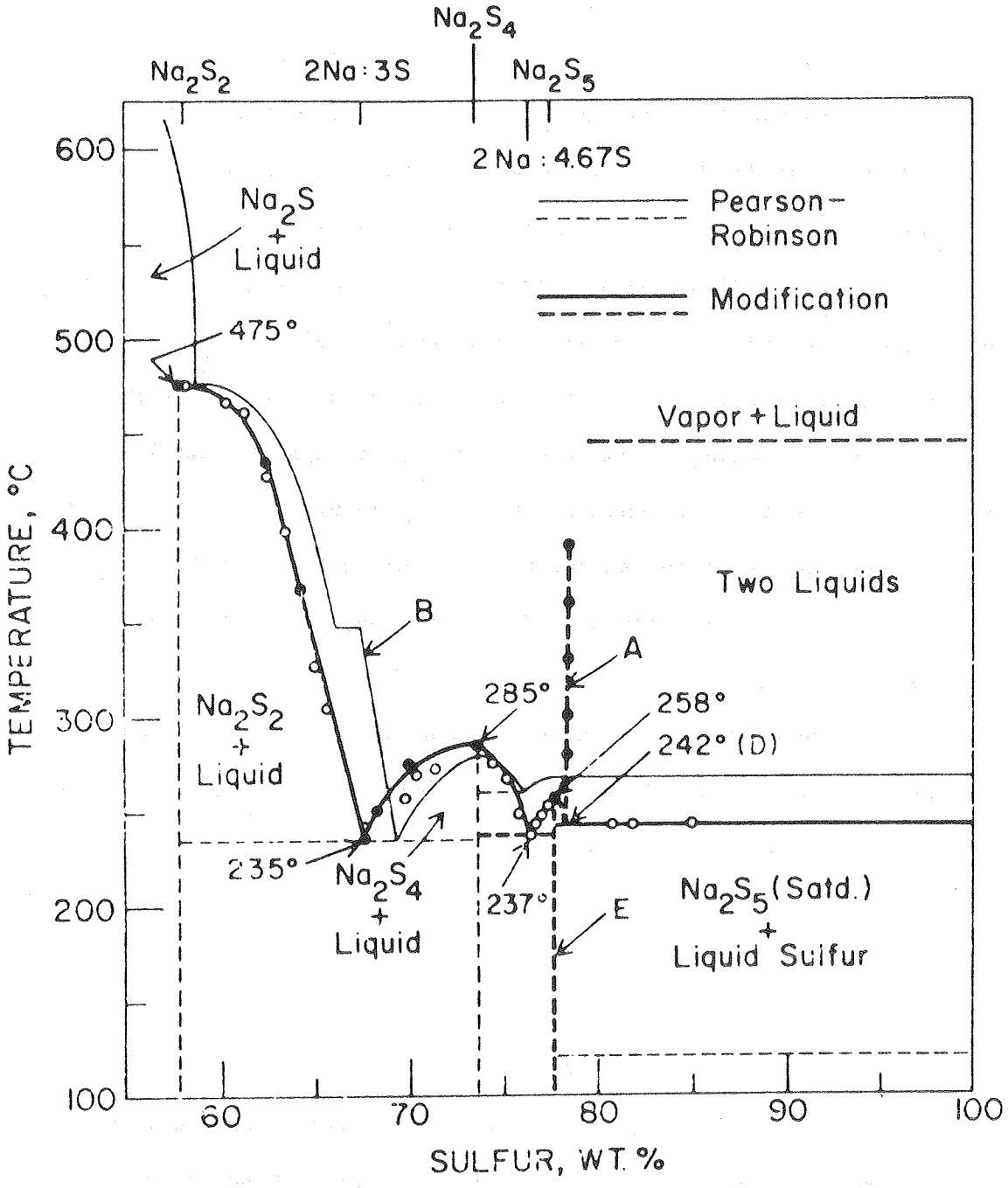

XBL 802-8074

FIGURE 4

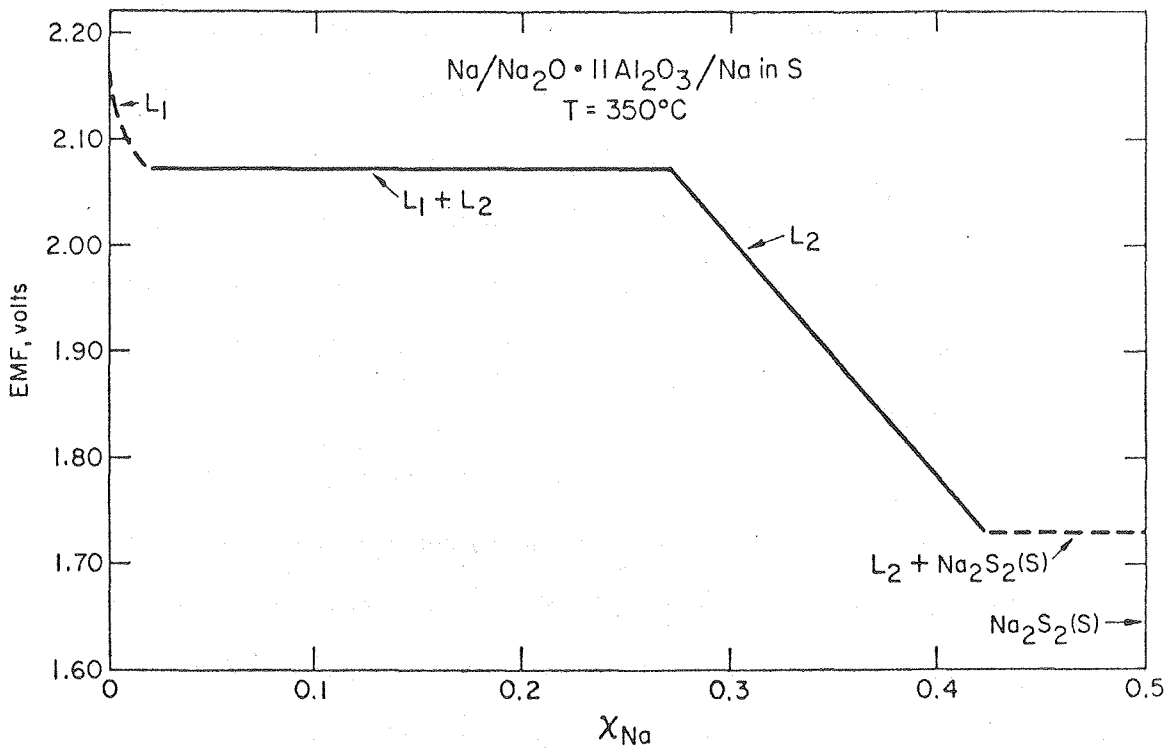
Na/Na2O • 11 Al2O3/Na in S
T = 350°C
L1
L1 + L2
L2
L2 + Na2S2(S)
Na2S2(S)
EMF, volts
2.20
2.10
2.00
1.90
1.80
1.70
1.60
0
0.1
0.2
0.3
0.4
0.5
XNa
XBL 801-7728

Na_2S_2 accumulates in the polysulfide melt until its solubility limit is reached, and solid Na_2S_2 precipitates at the electrolyte surface, preventing further reaction at a significant rate. The overall composition at this point is Na_2S_3 (at 350°C).

As the cell is recharged, the polysulfide phase is converted to sulfur which tends to form insulating layers, wetting and coating the graphite current collectors, preventing further reaction. This problem has resulted in a great deal of effort on improving the electronic conductivity of sulfur (by addition of such materials as C_6N_4), using specially shaped graphite felt current collectors,[6] and by tailoring the conductivity of the graphite current collector, in order to provide an optimized current distribution in the sulfur electrode, avoiding the blockage of the recharge process by insulating sulfur layers.

Most of the early Na/S cells were relatively small (tubes ∿1cm dia x 10-15 cm long, <15 Ah), and many had glass housings and seals. The problems of corrosion and impurities were studied in terms of their influence on cell resistance and lifetime. High purity sodium, free of potassium and other alkali metals is needed, to avoid cation exchange and cracking of the β-Al_2O_3. Impurities in the sulfur, such as Fe, Ni, etc., from corrosion of the steel cell case were found to cause problems with the sulfur electrode due to metal sulfide precipitation, blocking access of sulfur to the electrolyte. The corrosion of metal containers by sulfur remains a serious problem. Many coatings have been tested; chromium and molybdenum are among the best. Some borides are promising.

In spite of the various materials problems associated with the Na/β-Al_2O_3/S cell, the simplicity of the basic cell design and the low cost of the reactants have resulted in a wide-spread interest in this cell. Major

efforts exist in the U.S., England, France, Germany, and Japan. In the last few years, progress has been good, and a number of approaches are being taken to the problems. Cells of significantly more than 100 Ah capacity (typically, 165 Ah) have been tested, having electrolyte tubes of up to 3 cm diameter and 45-60 cm long. A recent design of a 168 Ah cell used by General Electric is shown in Figure 5.[7] This cell has sodium inside of the electrolyte tube, as do the Ford and Brown-Boveri cells. The cells of British Rail and Chloride Silent Power have sulfur inside the β''-Al_2O_3 tube, and sodium outside. This approach was taken to minimize the problem of corrosion by sulfur. Of course, the central current collector for the sulfur electrode must be corrosion resistant, but coatings are easier to apply to the outer surface of a current collector than to the inner surface of a cell case.

In all sodium/sulfur cells, the electrolyte tube is sealed to an alumina collar by a glass seal. This seal has been a cause of failure. Another difficult seal problem for this cell is that of the metal cell container to the alumina collar. Various gasketed seals with bolts have been used, but these are too heavy and expensive. Recently, emphasis has been placed upon thermocompression bonded seals, which appear to be more practical.

The internal resistance of the cells has a strong influence on the efficiency of operation, and the heat generation rate. In the interest of lowering the internal cell resistance to a value below 2 Ω-cm^2, a new sodium-ion electrolyte is being evaluated. This electrolyte, called NASICON, has an advantage of having high sodium ion mobility in all three crystallographic directions, rather than just two, as for β-Al_2O_3. The general formula for the family of NASICON compositions is $Na_{1+x}Zr_2Si_xP_{3-x}O_{12}$. Resistivities in the range of 2-4 ohm-cm have been reported at 300-350°C. Another problem with internal resistance in sodium/sulfur cells relate to the existence of a

FIGURE 5

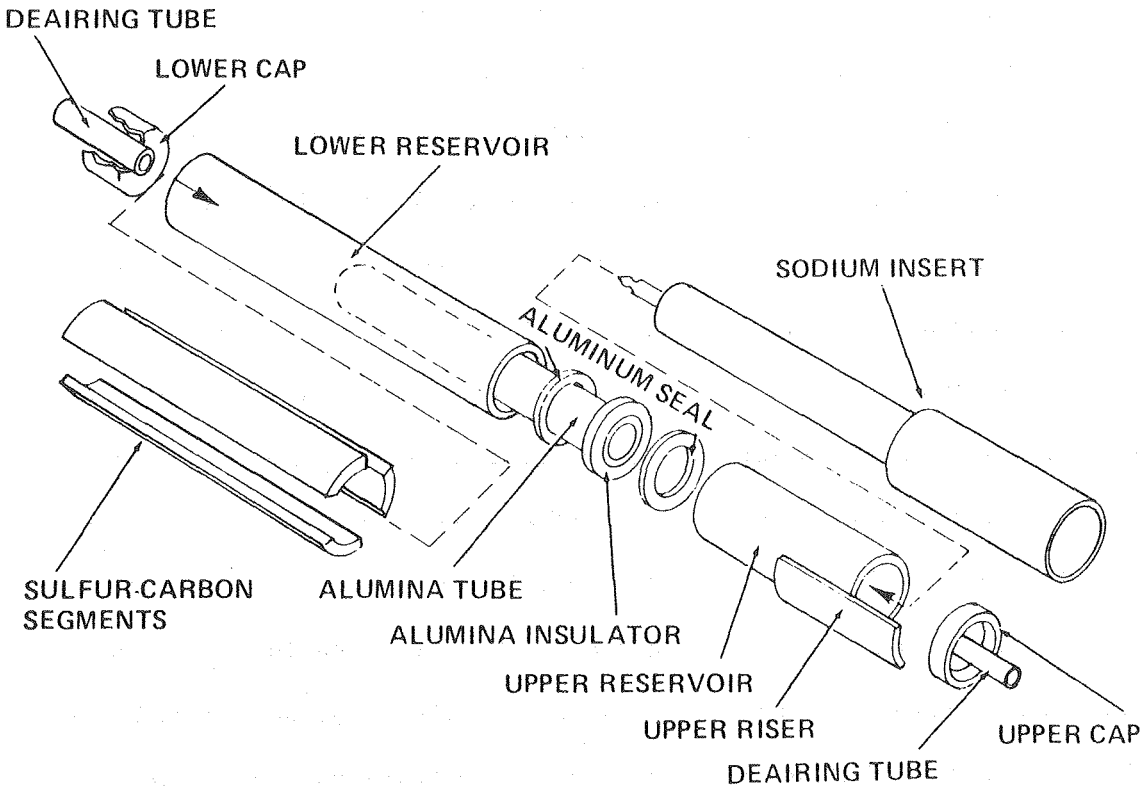

XBL 802-8070

resistance associated with the sodium/β"Al_2O_3 interface, which increases as cell cycling continues.[7] There is no general agreement on the precise source of this interfacial resistance, or means for eliminating it. The sulfur electrode, as one would expect, is a significant source of resistance. Various designs of graphite fiber current collectors have been investigated in attempts to reduce the cell internal resistance. Currently, the best values are about 2 Ω-cm^2, and 1.2 Ω-cm^2 may be achievable with present approaches (and electrolyte thicknesses near 1.5 mm).

Sodium/β-alumina/sulfur cells are typically operated at 350°C, a current density of 0.1 A/cm^2 or less, and have capacity densities of 0.2-0.4 Ah/cm^2, based on the area of the electrolyte. The resistance-area product for well-built cells is 2 ohm-cm^2 at 350°C. The specific energy values achieved by the best-designed cells are near 150 Wh/kg, at about 40 W/kg. There is a great deal of variation in the reported lifetimes of individual cells, but the better ones operate for more than 200 deep cycles; some have achieved about 1500 deep cycles.

A few multi-kilowatt-hour sodium/sulfur batteries have been tested, but their lifetimes have been very short, due to the variability of characteristics of the individual cells. The voltage-current curve for a 96-cell battery having a design capability of 10 kWh is shown in Figure 6.[8] The cells were arranged in four parallel strings, giving 50 V and 177 Ah. Currently, most of the sodium/sulfur battery programs are placing emphasis on semi-pilot production of cells having capacities of 100-200 Ah, the life-testing of these cells, and the preparation of batteries. The problems of thermal management and optimum interconnection of cells to form batteries are in the early stages of investigation. In the period 1980-82, a number of demonstration batteries for electric vehicles will be constructed and tested.

FIGURE 6

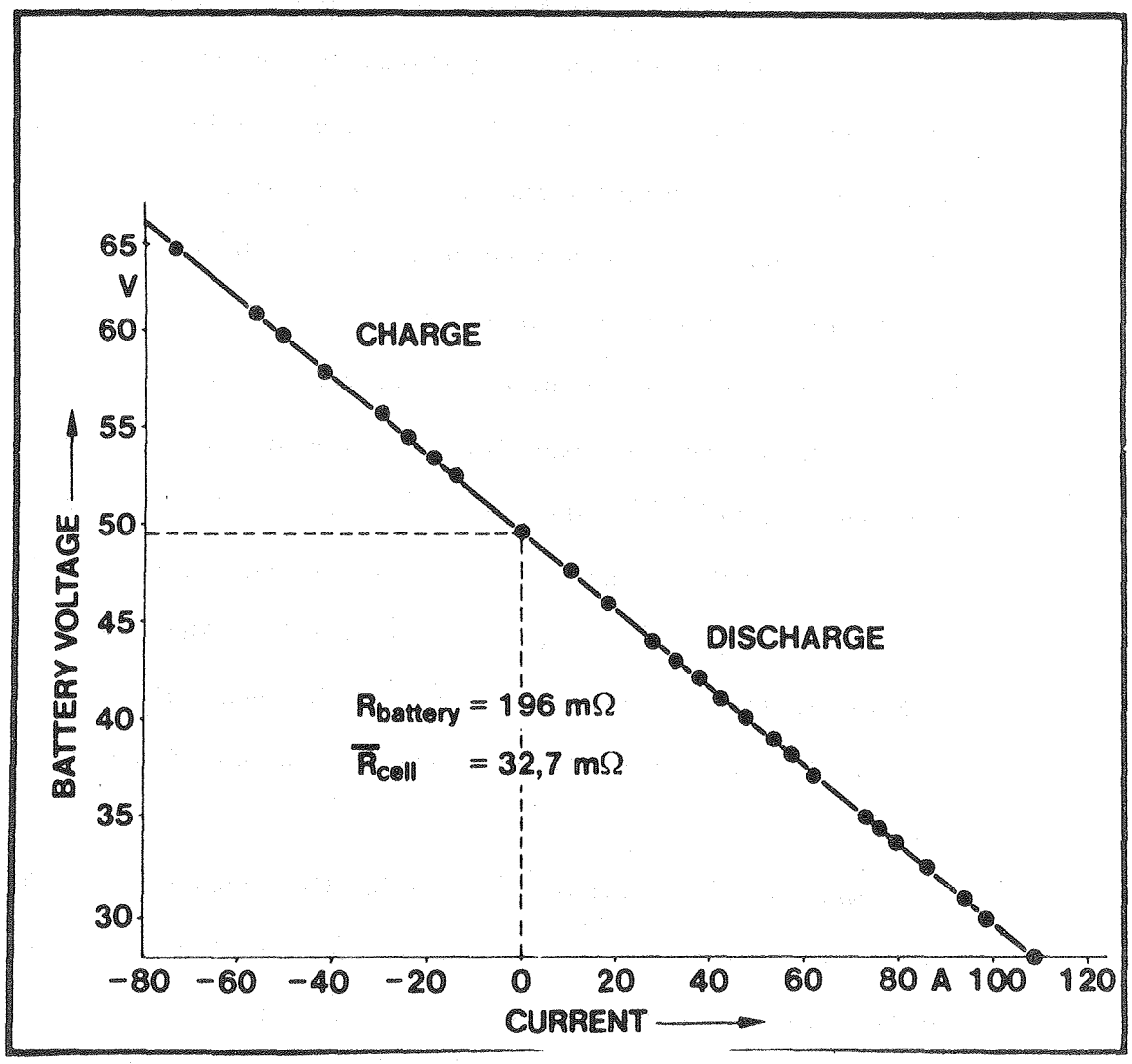

XBL 802-8071

Table 2 summarizes the present state of sodium/sulfur cell research and development. To put the status data into perspective, the best of the specific energy and specific power values are acceptable for energy storage and vehicle propulsion applications, as is the longest cycle life. The lifetime necessary for most applications is at least 3 years (26,000 h), and the cost should be below $100/kWh.

2.2 The Sodium/Sodium Glass/Sulfur Cell

This interesting cell operates according to the same principles as the sodium/beta alumina/sulfur cell. The beta alumina electrolyte, however, is replaced by a sodium-ion-conducting glass. This glass electrolyte has a much higher resistivity than beta alumina (10^4 Ω-cm vs. 3-20 Ω-cm at 300-350°C). It is necessary, therefore, to use a much thinner layer of electrolyte between the electrodes, and to operate the cell at much lower current densities in order to have an acceptably small voltage loss due to the cell resistance. This is accomplished by using hollow fibers of glass electrolyte, 70 μm O.D., and 50 μm I.D., with a 10 μm wall thickness.

The design of the sodium/sodium glass/sulfur cell, using thousands of hollow glass fibers is shown in Figure 7.[9] The fibers have one end sealed, and the other (open) end bonded to a glass tubesheet, providing communication between the insides of the fibers and the sodium reservoir. The sulfur is on the outsides of the hollow fibers. Current collection in the sulfur electrode is provided by a carbon- or molybdenum-coated aluminum foil which is spirally wound among the glass fibers (a simple operation performed by rolling the fibers together with the Al foil before sealing into the tubesheet). Typically, the distance between fibers is 200 to 500 μm, and the distance from a fiber to the Al current collector is 20 μm. Because of the very large total electrolyte area offered by the fibers, the operating current density

TABLE 2

$Na/\beta-Al_2O_3/S$

$2Na + 3S \rightarrow Na_2S_3$

$\bar{E}$ = 2.0 V; 758 Wh/kg Theoretical

Status

Cell Size	50-200 Ah
Specific Energy	85-150 Wh/kg @ 30-40 W/kg
Specific Power	60-130 W/kg peak
Cycle Life	200-1500
Lifetime	3000-15,000 h
Cost	>$1000/kWh

Recent Work

Batteries, ∿10 kWh

C_6N_4 additive to S

Ceramic (TiO_2) electronic conductors

Shaped current collectors

Tailored resistance current collectors

Sulfur-core cells

$Na_{1+x}Zr_2Si_xP_{3-x}O_{12}$

Thermocompression bonded seals

Problems

High $Na/\beta''-Al_2O_3$ interfacial resistance

Corrosion of materials in contact with S

High cost seals

High cost electrolyte

Thermal cycling causes failure

Thermal control of batteries

Cell mismatch in batteries

FIGURE 7

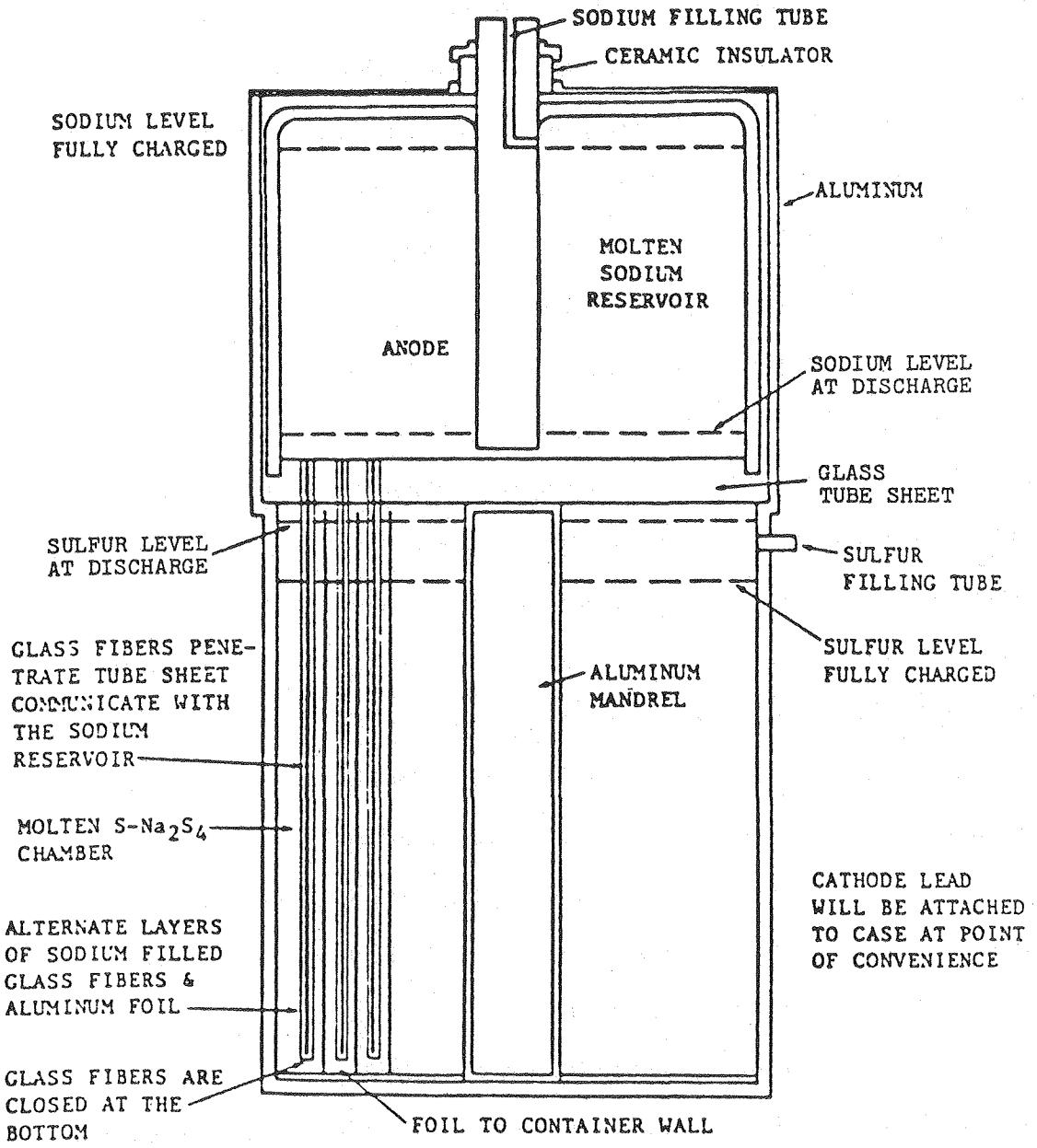

XBL 7912-13726

is only 0.002 A/cm^2, yielding a low resistance loss (0.1 V), and a high efficiency (typically, 90% overall). This cell is designed to operate at 300°C between the composition limits Na_2S_{20} (charged) and $Na_2S_{3.5}$ (discharged), with a theoretical specific energy of 691 Wh/kg. A sulfur utilization of 90% (based on $Na_2S_{3.5}$) is achieved. As expected, the cell resistance rises rapidly toward the end of the charging process. Many small cells (0.5 to 6 Ah*) have been tested, and lifetimes up to about 9000 hr, and 500 cycles have been achieved with stable performance. A small number of 40 Ah cells (with 13,000 fibers) have been tested also.

The current problems with the glass fiber cell include fracture of the fibers near the tubesheet, gradual sagging of the glass tubesheet, and undesirable interaction between the two glass compositions making up the fibers and the tubesheet. When a number of fibers fail, the exothermic reaction between sodium and sulfur can cause thermal runaway. This safety problem is currently receiving attention. Thermal control must be reasonably precise for these cells because the cell resistance (mostly glass fiber resistance) has a high temperature coefficient. Cooldown of cells after startup is not permitted, because of excessive fiber breakage.

Recent work with 40 Ah cells is encouraging, and development of these cells continues, with emphasis on increasing cell lifetime and improved safety. Table 3 presents a summary of the status of this cell.

2.3 The Sodium/Beta-Alumina/Antimony Trichloride Cell

This cell is a relative of the sodium/sulfur cells. It uses a molten salt mixture of $SbCl_3$ in $NaCl-AlCl_3$ in place of sulfur as the positive electrode reactant. The melting point of $NaCl-AlCl_3$ mixtures is low enough that cell operation can be carried out at 200°C. It was claimed by the

*The 6 Ah cells contain about 2000 fibers.

TABLE 3

Na/Na glass/S

$2\ Na + 3.5S \rightarrow Na_2S_{3.5}$

$\bar{E} = 2.0\ V;\ 691\ Wh/kg$

Status

Cell Sizes	0.5, 6, 40 Ah
Specific Energy	n.a.
Specific Power	n.a.
Cycle Life	500
Lifetime	9000 h
Cost	>$1000/kWh

Recent Work

- 40 Ah Cells
- Mo coating on Al
- New glass for tubesheet
- Safety

Problems

- Breakage of fibers near tubesheet
- Thermal runaway on failure
- Sagging of tubesheet
- Compatibility of fibers and tubesheet
- Impurities attack fibers
- High temperature coefficient of resistance
- Thermal cycling

TABLE 4

$Na/\beta''\text{-}Al_2O_3/SbCl_3$ in $AlCl_3$

$3Na + SbCl_3 + 3AlCl_3 \rightarrow 3NaAlCl_4 + Sb$

$\bar{E}$ = 2.8 V; 328 Wh/kg Theoretical

Status

Specific Energy (projected)	90 Wh/kg @ 12 W/kg
Specific Power (projected)	30 W/kg
Cycle Life	100 @ 100% DOD
Cost	too early
Operating Temperature	210°C

Recent Work

Tubular cells	6 Ah, 30 Ah
Improved electrode designs	

Problems

- Wetting of $\beta''\text{-}Al_2O_3$ by Na
- Current collectors (W or Mo)
- Seals
- Low current density ($7.5 mA/cm^2$)
- Degradation of $\beta''\text{-}Al_2O_3$
- Slow recharge (14 h)
- Low specific energy

investigators[10,11,12] that the lower operating temperature would permit polymeric materials to be used as insulators and seals, however, these were not satisfactorily developed and demonstrated.

The overall cell reaction is as follows:

$$3Na + SbCl_3 + 3AlCl_3 \rightarrow 3NaAlCl_4 + Sb \quad (9)$$

With an average cell potential of 2.8 V, the theoretical specific energy is 328 Wh/kg.

Small cells, up to 6Ah, were operated at current densities up to 7.5 mA/cm^2. These cells used graphite powder and molybdenum or tungsten as the current collector in the positive electrode. Cycle lives of about 100 have been demonstrated. Problems encountered in the work on this cell have included difficulty of wetting of the β''-Al_2O_3 by sodium, inadequate seals, low current density, and degradation of the β''-Al_2O_3.

The status of this cell is shown in Table 4 where a projected specific energy of 90 Wh/kg is given. This value is low, compared to the values already demonstrated for the Na/S cell (150 Wh/kg).

2.4 The Sodium/Beta-Alumina/Sulfur Chloride Cell

The newest cell of the sodium/beta alumina family of cells uses SCl_4 in NaCl-$AlCl_3$ as the positive electrode reactant.[13] Again, a lower operating temperature is offered by the NaCl-$AlCl_3$ mixture: temperatures of 130 to 255°C have been used.

The overall cell reaction for reduction to S° is:

$$4Na + SCl_3AlCl_4 + 3AlCl_3 \rightarrow S + 4NaAlCl_4 \quad (10)$$

The cell voltage is impressively high: 4.2 V; yielding a theoretical specific energy for Reaction 10 of 563 Wh/kg.

Some glass laboratory cells have been operated according to Reaction 10, having a capacity of 4 Ah at 255°C.[13] These cells have used tungsten

spiral current collectors, and have operated for at least 45 cycles before failure of the β''-Al_2O_3 electrolyte.

The status of the work on the Na/β''-Al_2O_3/SCl_4 in NaCl-$AlCl_3$ cell is shown in Table 5. The high cell voltage offers the possibility of high efficiency. If the S° can be reduced to $S^{=}$ by deeper discharge at a voltage above about 3 V, the specific energy in practical cells could be well above 100 Wh/kg.

3. CELLS WITH MOLTEN SALT ELECTROLYTES

All of the rechargeable cells with molten salt electrolytes currently under development make use of solid electrodes. These cells are an outgrowth of earlier work on cells with liquid electrodes and molten salt electrolytes.[14,15,16] The forerunner of the present Li alloy/molten salt/FeS_x cells was the Li/LiCl-KCl/S cell,[15,16] which was very attractive because of its high theoretical specific energy (2600 Wh/kg) and attractive cell potential (~2.4 V). Significant problems with the solubility of polysulfides in the electrolyte, and the retention of liquid lithium in its current collector caused attention to be focused upon immobilization of lithium in the form of a solid alloy (of relatively high lithium activity) and the insolubilization of sulfur and polysulfides by using transition metal sulfides (which have a very low solubility). These measures cause a significant decrease in the specific energy of the cell and a moderate decrease in voltage, but a great increase in cell lifetime.

In principle there are many lithium alloys that can be used as the negative electrode, but only a few of them have an acceptable combination of low weight per electrochemical equivalent, low cost, ability to be recharged many times, high exchange current density, and high lithium diffusion coefficient. The alloys that have been investigated most are Li-Al[17,18] and Li-Si.[19,20]

TABLE 5

$Na/Na_2O \cdot xAl_2O_3/SCl_3AlCl_4$ in $AlCl_3$-NaCl T = 250°C

$$4Na + SCl_3AlCl_4 + 3AlCl_3 \rightarrow 4NaCl \cdot AlCl_3 + S$$

E = 4.2 V; 563 Wh/kg Theoretical

Status: glass lab cells only (4 Ah)

Current Density	20 mA/cm^2 @ 3.5 V
Power Density	150 mW/cm^2 max. @ 2.5 V
Cycle Life	45 @ 100% DOD
Cost	too early

Recent Work

Larger cells - 4 Ah

Less expensive current collectors

Problems

Sodium wetting

Vapor pressure

Corrosion of metals and some electrolytes

Electrolyte cracking

Overcharge ?

Some recent work has been performed with Ca-Si and other calcium alloys.[21,22]

The metal sulfides that have been investigated as positive electrodes include the iron sulfides, nickel sulfides, cobalt sulfides, copper sulfides, and molybdenum sulfide.[23] The ones receiving the most emphasis are FeS and FeS_2.

From the several negative and positive electrode materials indicated above, a long list of cells can be made, however only two of these have been receiving a significant amount of research and development effort. These are LiAl/LiCl-KCl/FeS, Li_4Si/LiCl-KCl/FeS_2. Another system of interest is Ca_2Si/LiCl-NaCl-$CaCl_2$-$BaCl_2$/FeS_2.

3.1 The Lithium-Aluminum/Lithium Chloride-Potassium Chloride/Iron Monosulfide Cell

This electrochemical system has shown itself to be very stable in operation, with relatively few serious operating and materials problems. The overall cell reaction is:

$$2LiAl + FeS \rightarrow Li_2S + Fe + 2Al \qquad (11)$$

This cell is usually operated at 450°C, and exhibits a single voltage plateau near 1.3 V, as shown in the constant current discharge curves of Figure 8.[24] The overall reaction given above, and the single voltage plateau are, however, misleadingly simple. Detailed investigations of the phase transformations occurring during charge and discharge of the FeS electrode have led to the establishment of the phase diagram shown in Figure 9.[22]

The dashed line C-D in Figure 9 shows the path followed by the composition of the FeS electrode from the fully charged condition (point C) to the fully discharged condition (point D). Starting at point C, as lithium is added to the FeS electrode by electrochemical reaction, two new phases, Li_2FeS_2 and Fe, are formed:

FIGURE 8

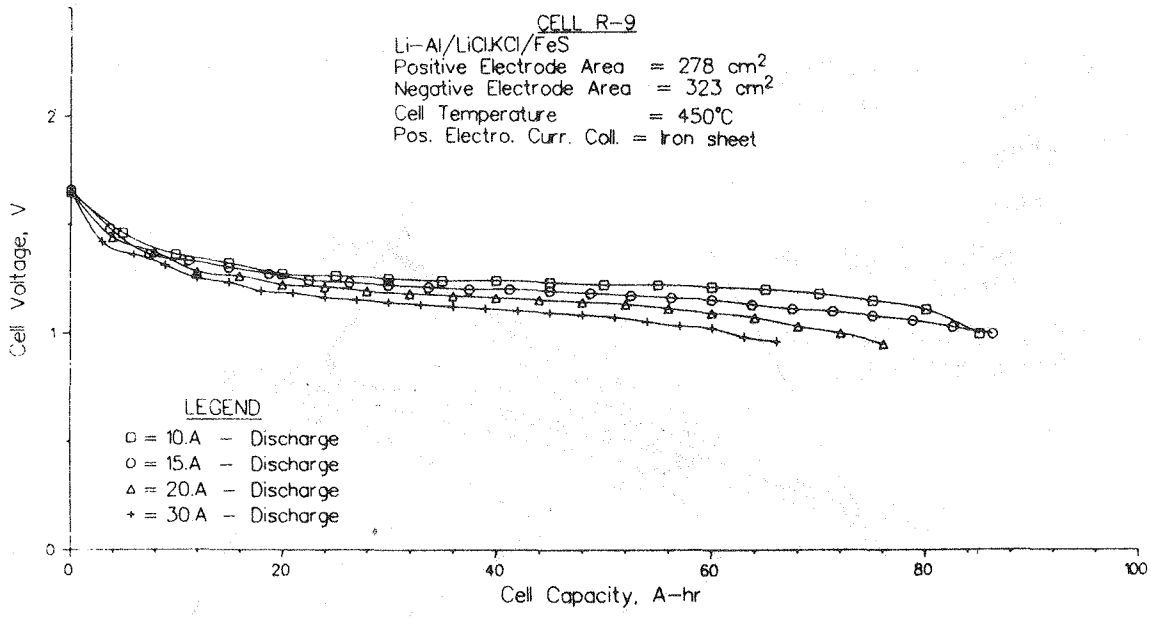

XBL 802-8069

FIGURE 9

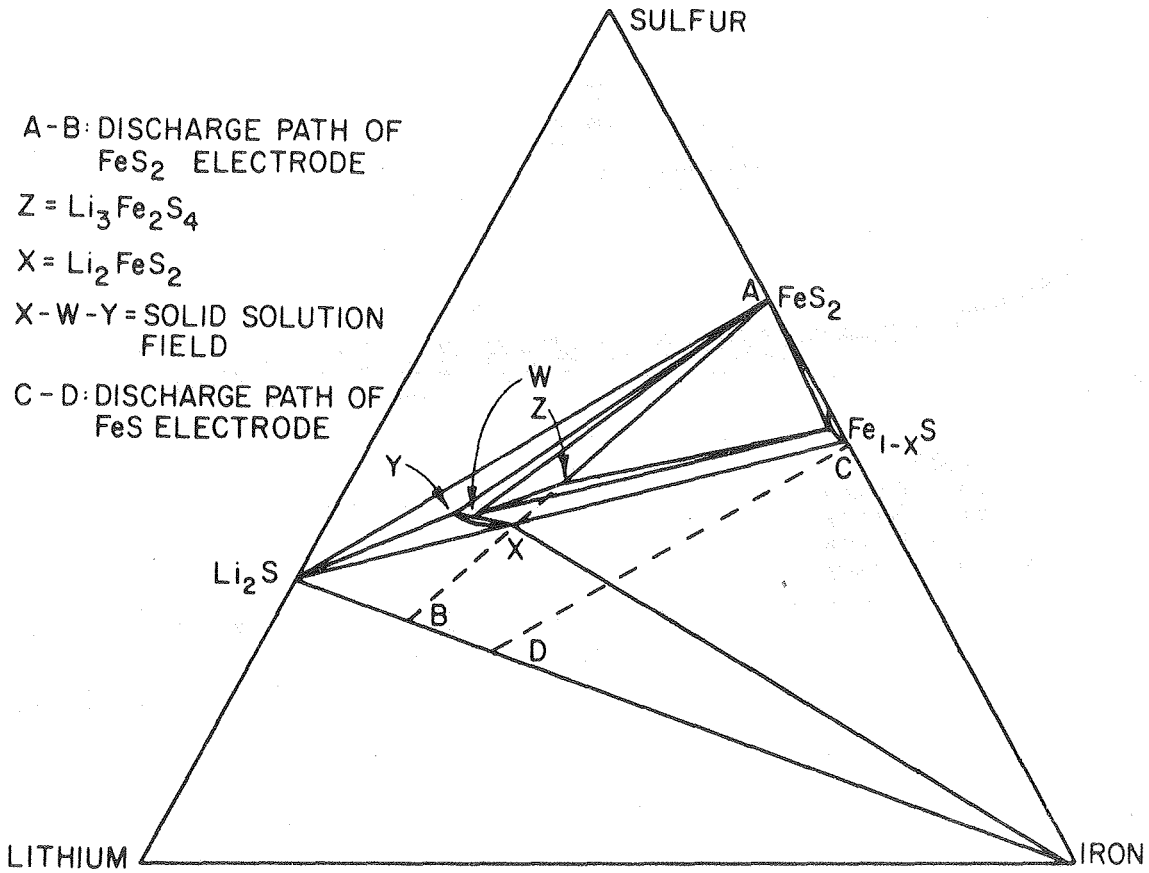

XBL 802-8072

$$2FeS + 2Li \rightarrow Li_2FeS_2 + Fe \quad (12)$$

Additional discharge beyond the point where line C-D crosses the X-Fe line in Figure 9 results in a new phase, Li_2S, being formed:

$$Li_2FeS_2 + 2Li \rightarrow 2Li_2S + Fe \quad (13)$$

Reactions 12 and 13 occur at essentially the same potential, near 1.6 V vs. reversible lithium, so the voltage vs. capacity curve for the discharge from point C to point D shows only one plateau.

Depending on the temperature of operation, and the composition of the LiCl-KCl electrolyte, another phase, called djerfischerite, may form, having the composition $LiK_6Fe_{24}S_{26}Cl$.[22] This material tends to reduce the rate at which the recharge reactions can be carried out, hence its formation is undesirable. The extent of formation of $LiK_6Fe_{24}S_{26}Cl$ can be minimized by using an electrolyte that has more LiCl than the eutectic composition, and by operating at temperatures above 450°C.[25]

The negative electrode for the LiAl/FeS cell is the intermetallic compound LiAl, which has a potential 0.3 V positive with respect to a reversible pure lithium electrode. The phase diagram of Figure 10[26] shows that there is a broad composition range (from 10% to 45% Li in Al) over which there is a two-phase mixture ($\beta+\alpha$), yielding a single voltage plateau (0.3 V vs. reversible Li). This feature makes the Li-Al electrode attractive.

Lithium/iron monosulfide cells of various designs have been constructed and tested. A multiplate cell with two positive (FeS) and three negative (LiAl) electrodes is shown in Figure 11.[23] The electrodes for such cells may be prepared by various techniques, including cold or hot pressing of mixed powders of reactant and electrolyte (with or without a current collector powder such as graphite for the FeS added), or by using a conductive carbon cement (the so-called carbon bonded structure). Various

FIGURE 10

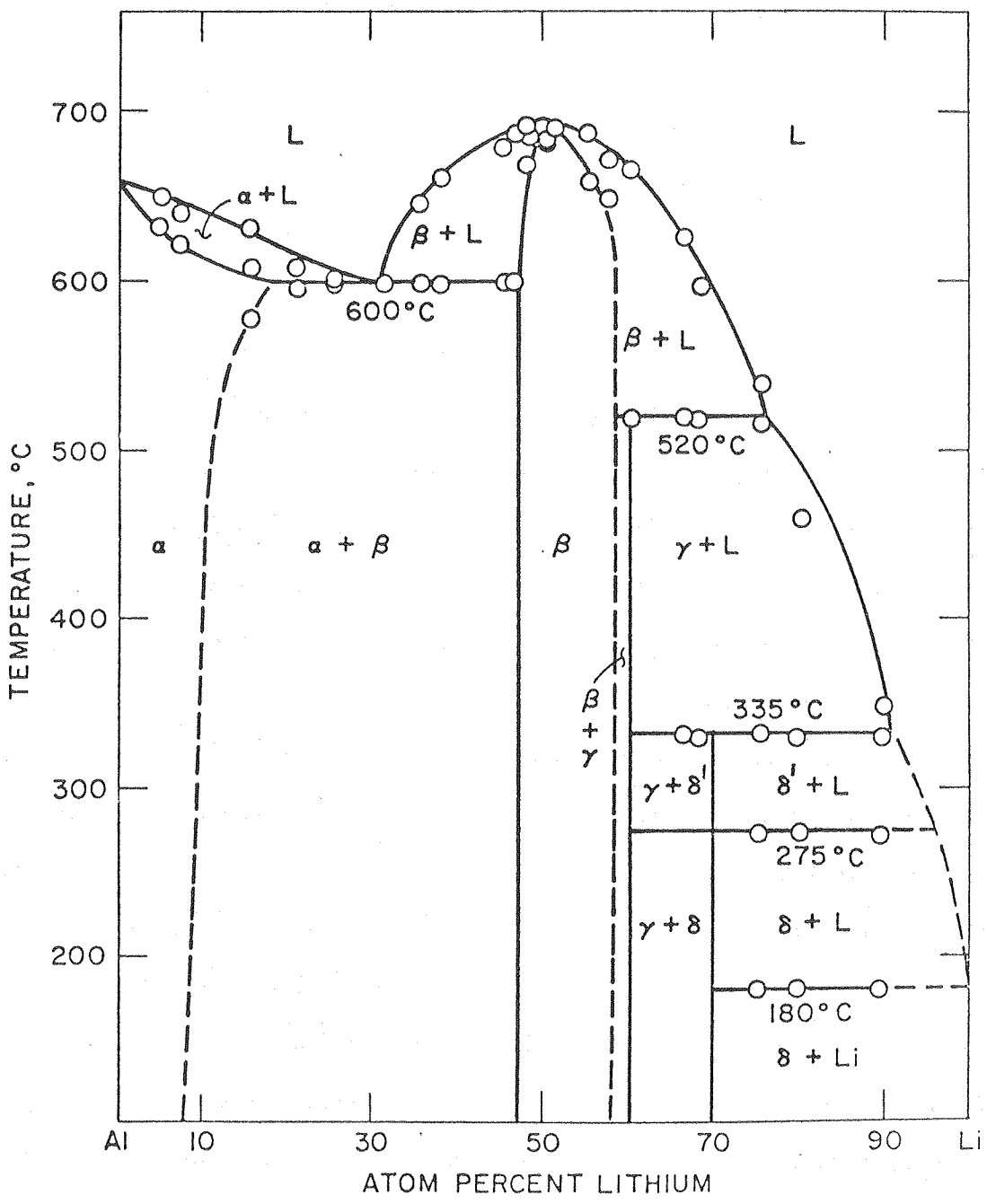

(α = Al, β = LiAl, γ = Li_3Al_2, δ = δ' = Li_9Al_4)

XBL 801-7726

FIGURE 11

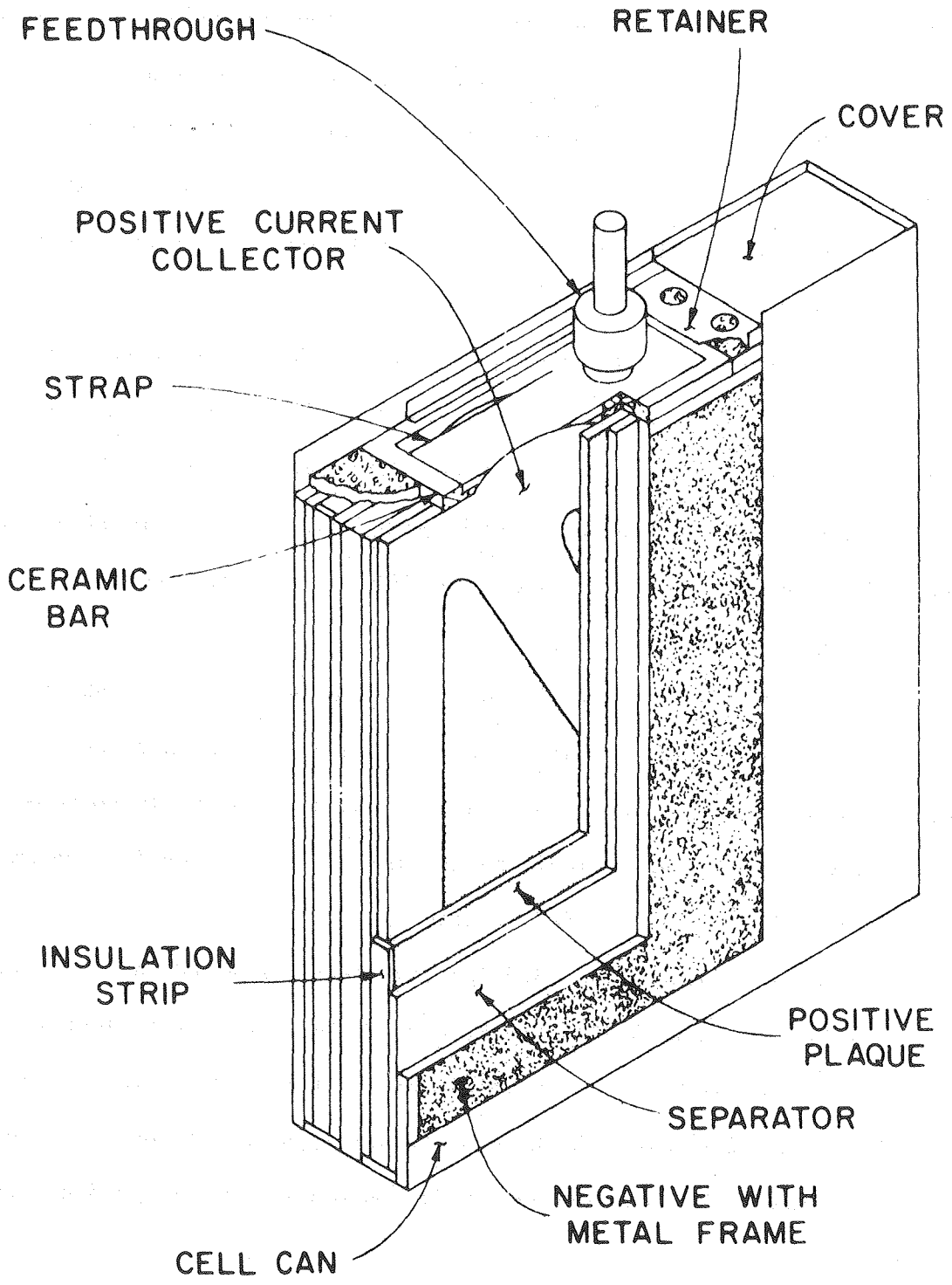

XBL 802-8073

additives to the FeS electrode have been used to improve the utilization and current collection, including Cu_2S (about 6 m/o). The current collectors are made of corrosion-resistant metals such as iron, iron alloys, stainless steels, etc. The electrolyte is soaked into a porous boron nitride mat, which may be a woven cloth or a felt. The boron nitride is not readily wetted by the LiCl-KCl electrolyte. Wettability is improved by the addition of $LiAlCl_4$ to the BN mat ($\sim$20 mg/cm^2).

Cells of the general multiplate type described above have been evaluated with regard to performance and lifetime. Figure 12[27] shows the specific energy vs. cycle number data of some 300 Ah cells designed for use in electric vehicles. Specific energies near 100 Wh/kg were achieved early in life (vs. 458 Wh/kg theoretical). Cycle lives of over 300 were achieved before 40% of the initial specific energy was lost.

Failure modes for these cells include shorting due to active material from the positive electrode extruding through openings in the structure, and touching the negative electrode. The gradual loss of capacity is to some degree associated with morphological changes in the Li-Al alloy (an agglomeration of the initially finely divided structure).

Cells of the multiplate type (300 Ah) have been assembled into batteries, including a module for a fork-lift truck, and 20 kWh modules for electric van testing. Initial results for the 10 cell* fork-lift battery are shown in Figure 13.[27] The 20 kWh modules have had start-up problems; more will be tested. Experience with batteries and their thermal control is needed very much.

Table 6 summarizes the status of the LiAl/FeS cell. The current problems include a relatively low specific energy, internal cell shorting and

*Two parallel strings of 5 ladder-connected cells.

TABLE 6

LiAl/LiCl-KCl/FeS

$2LiAl + FeS \rightarrow Li_2S + Fe + 2Al$

E = 1.33 V; 458 Wh/kg Theoretical

Status

Cell Size	320 Ah
Specific Energy	50-90 Wh/kg @ 30 W/kg
Specific Power	60-100 W/kg, peak
Cycle Life	300 @ 100% DOD
Lifetime	∿5000 + h
Cost	>$1000/kWh

Recent Work

- Multielectrode cells
- LiCl-rich electrolyte
- BN felt separators
- Batteries of 320 Ah cells
- Charging equipment

Problems

- Low specific energy
- Low voltage per cell
- Cell shorting major failure made
- Electrolyte leakage
- Agglomeration of Li-Al with cycling
- High separator cost
- Leak-free feedthroughs
- Thermal control

FIGURE 12

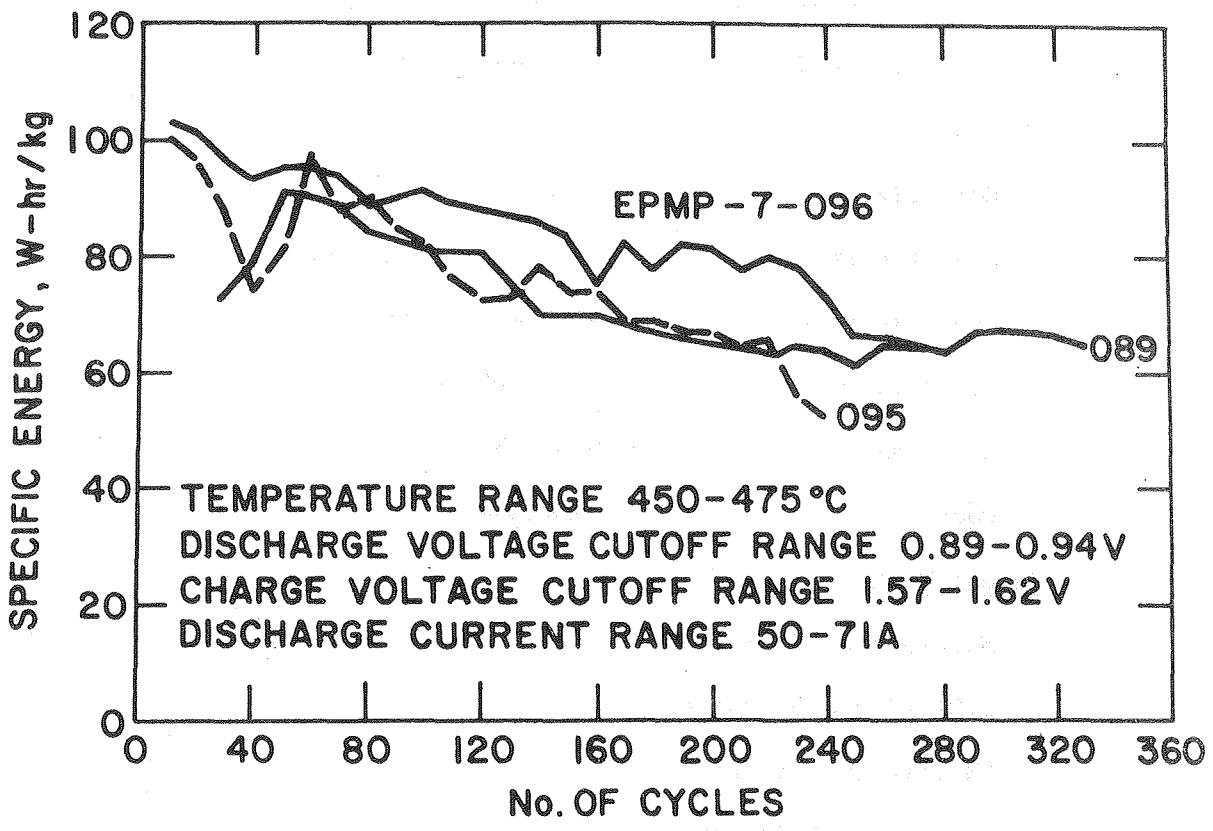

XBL 801-7729

FIGURE 13

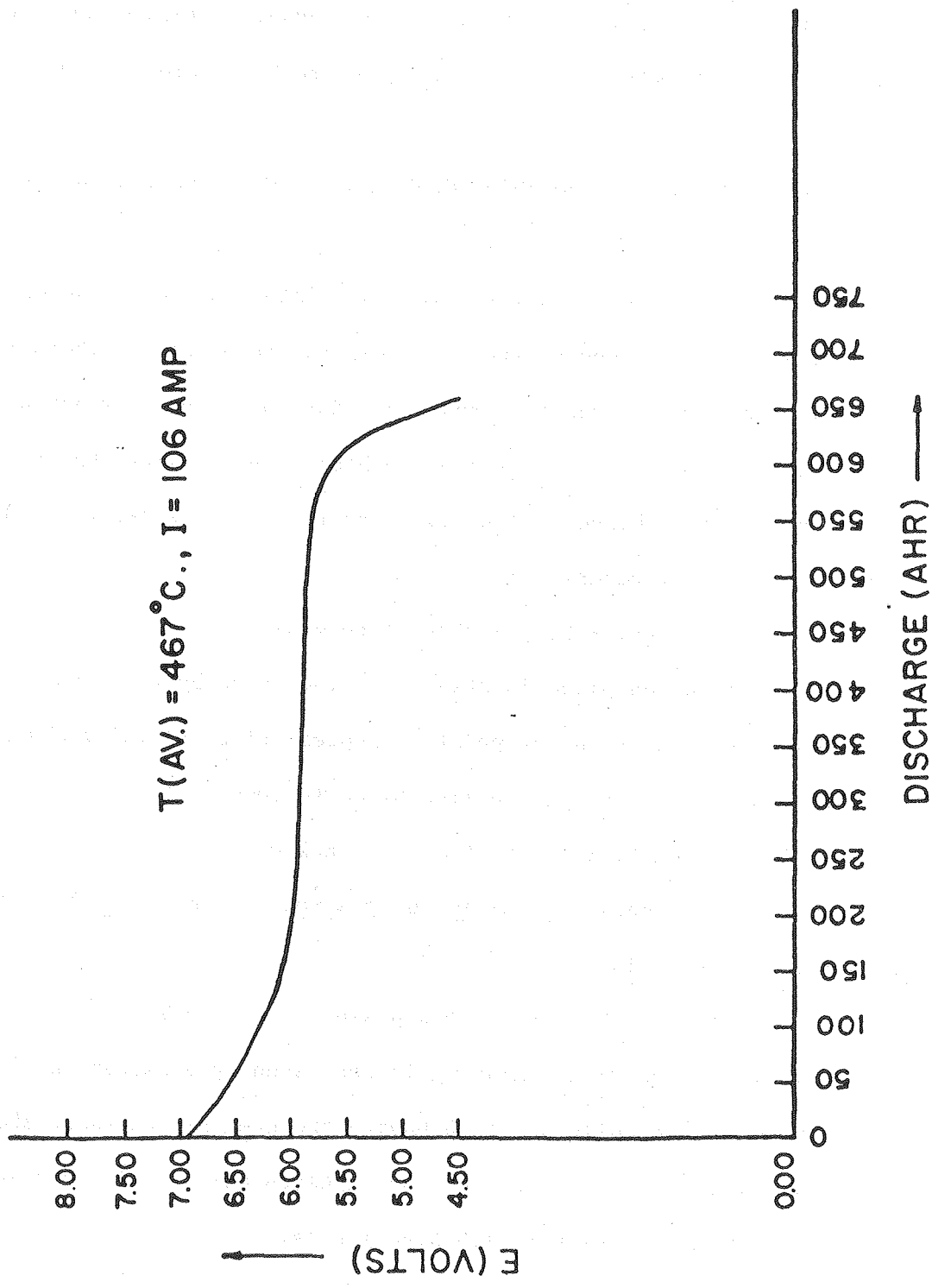

XBL 7912-13727

high cost of BN separators. Sufficient promise has been shown by the results that industrial organizations are constructing pilot quantities of cells for testing and demonstration, under government sponsorship. This system may be the first to achieve commercial status among the rechargeable cells with molten salt electrolyte.

3.2 The Lithium-Silicon/Lithium Chloride-Potassium Chloride/Iron Disulfide Cell

This electrochemical cell is very closely related to the one described immediately above and operates at the same temperature (450°C). The main difference is that both the positive and the negative electrode reactants have significantly lower weights per electrochemical equivalent than those of the LiAl/FeS cell. The theoretical specific energy is 944 Wh/kg vs. 458 Wh/kg. The overall cell reaction is:

$$Li_4Si + FeS_2 \rightarrow 2Li_2S + Fe + Si \qquad (14)$$

Reaction 14 actually takes place in stages, as indicated by the path A-Z-X-B in Figure 9. Starting at point A, representing the fully-charged positive electrode, FeS_2 reacts with lithium as follows:[27]

$$2FeS_2 + 3Li \rightarrow Li_3Fe_2S_4 \qquad E=2.04\ V \qquad (15)$$

This is followed by a reaction involving only a few percent (∿4.5%) of the total charge of Reaction 14:

$$Li_3Fe_2S_4 + Li \rightarrow Fe_{1-x} + \text{W-phase} \qquad E=1.9\ V \qquad (16)$$

Reaction 16 is not balanced; its meaning is best seen by examination of Figure 9. W-phase is a solid solution having the composition range shown in Figure 9. The next stage of reaction also involves only a small portion (∿8.25%) of the charge associated with Reaction 14:

$$Fe_{1-x}S + W + Li \rightarrow Li_2FeS_2 \qquad E=1.9\text{-}1.64\ V \qquad (17)$$

The final step is:

$$2Li_2FeS_2 + 4Li \rightarrow 4Li_2S + 2Fe \qquad E=1.64\ V \qquad (18)$$

Note that out of an overall 8-electron process for Reactions 15 through 18, only one electron is associated with the sum of Reactions 16 and 17. The reaction scheme above, proposed by Tomczuk and Martin[27] is based upon extensive phase diagram work, voltage sweep experiments, and metallographic work on electrodes operated under well controlled conditions, as well as electrodes from engineering cells.

The negative electrode, Li-Si, operates according to the phase diagram of Figure 14.[20] This electrode is operated between the extremes of silicon and Li_4Si. The phases encountered at 450°C are: Si, Li_2Si, $Li_{21}Si_8$, $Li_{15}Si_4$, and $Li_{22}Si_5$, and the voltage plateaus (vs. reversible lithium) are given in Table 7.[20]

It is obvious that the combination of the FeS_2 electrode with two major plateaus and the Li-Si electrode with perhaps three major plateaus will yield a complex voltage vs. capacity curve for the complete cell showing several plateaus.

A cross-section of a typical light-weight development cell using Li_4Si and FeS_2 electrodes is shown in Figure 15.[23] This cell is in the form of a circular disc, with a central positive electrode, and two negative electrodes. The electrodes are separated by a BN cloth or felt. The electrodes may be prepared by various techniques, including pressing of powder mixtures into the desired shapes. The specific energy vs. specific power curves for two cells of this type are shown in Figure 16.[23] Note that specific energies above 180 Wh/kg have been achieved at low specific power, and that specific powers up to about 100 W/kg have been demonstrated also. This is in contrast to the lower specific energy of the LiAl/FeS cell ($\sim$100 W/kg).

Life testing of Li_4Si/FeS_2 cells has shown that cycle lives of 700

TABLE 7

EMF Values for the Li-Si Electrode at 725°K

Phases in Equilibrium	EMF vs. Li
$Si-Li_2Si$	0.326
$Li_2Si-Li_{21}Si_8$	0.277
$Li_{21}Si_8-Li_{15}Si_4$	0.149
$Li_{15}Si_4-Li_{22}Si_5$	0.042
$Li_{22}Si_5$-Li (Sat. with Si)	0.001

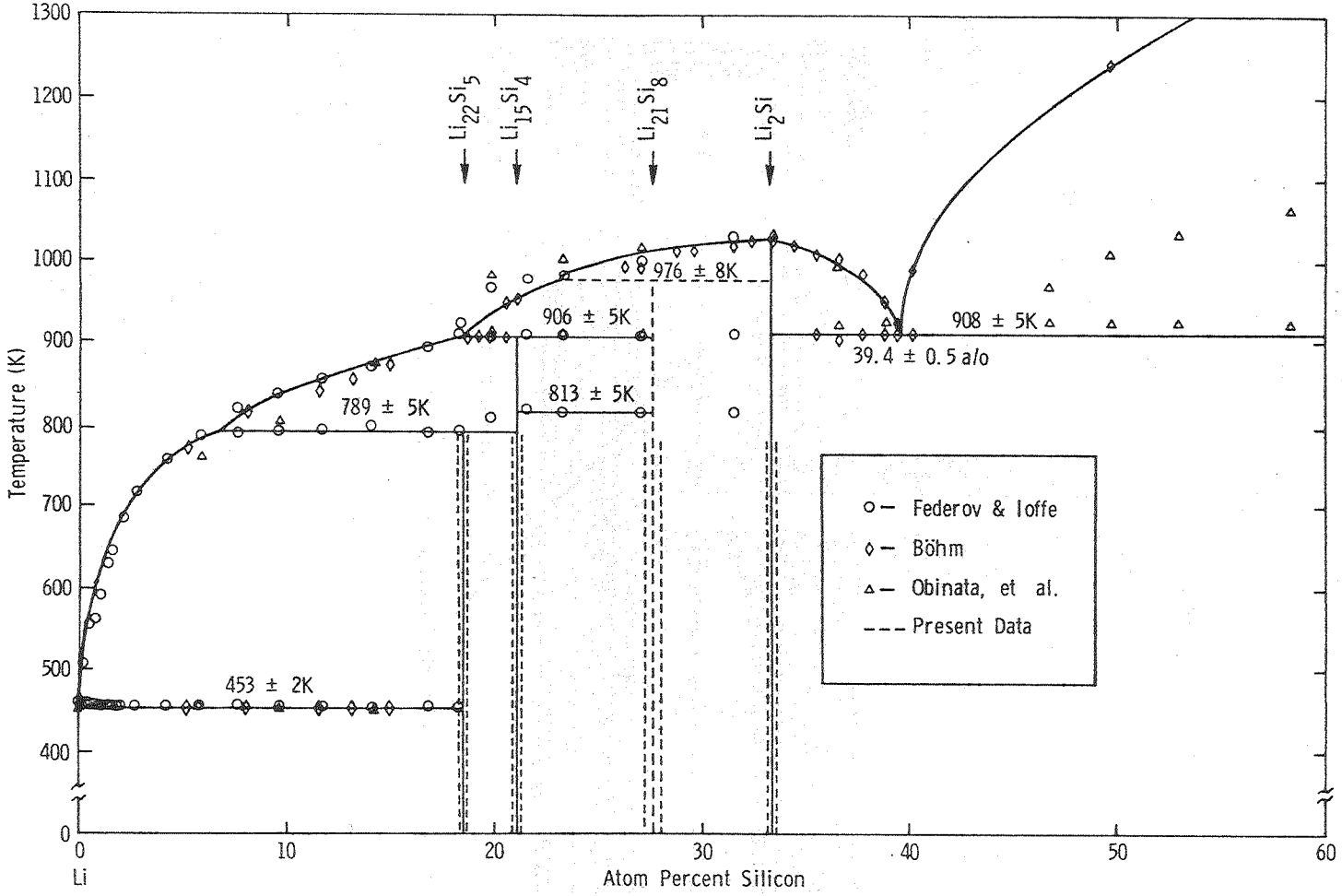

XBL 801-7727

FIGURE 14

FIGURE 15

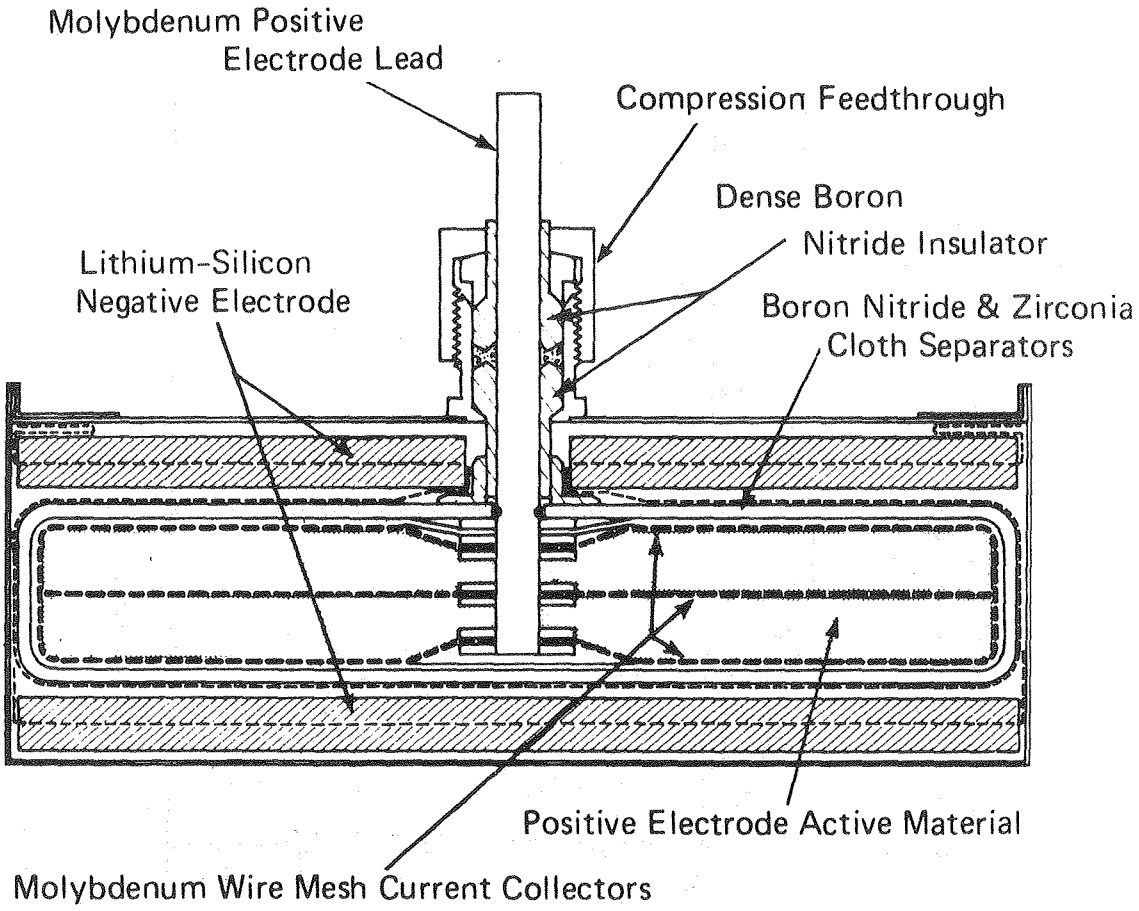

XBL 802-8075

FIGURE 16

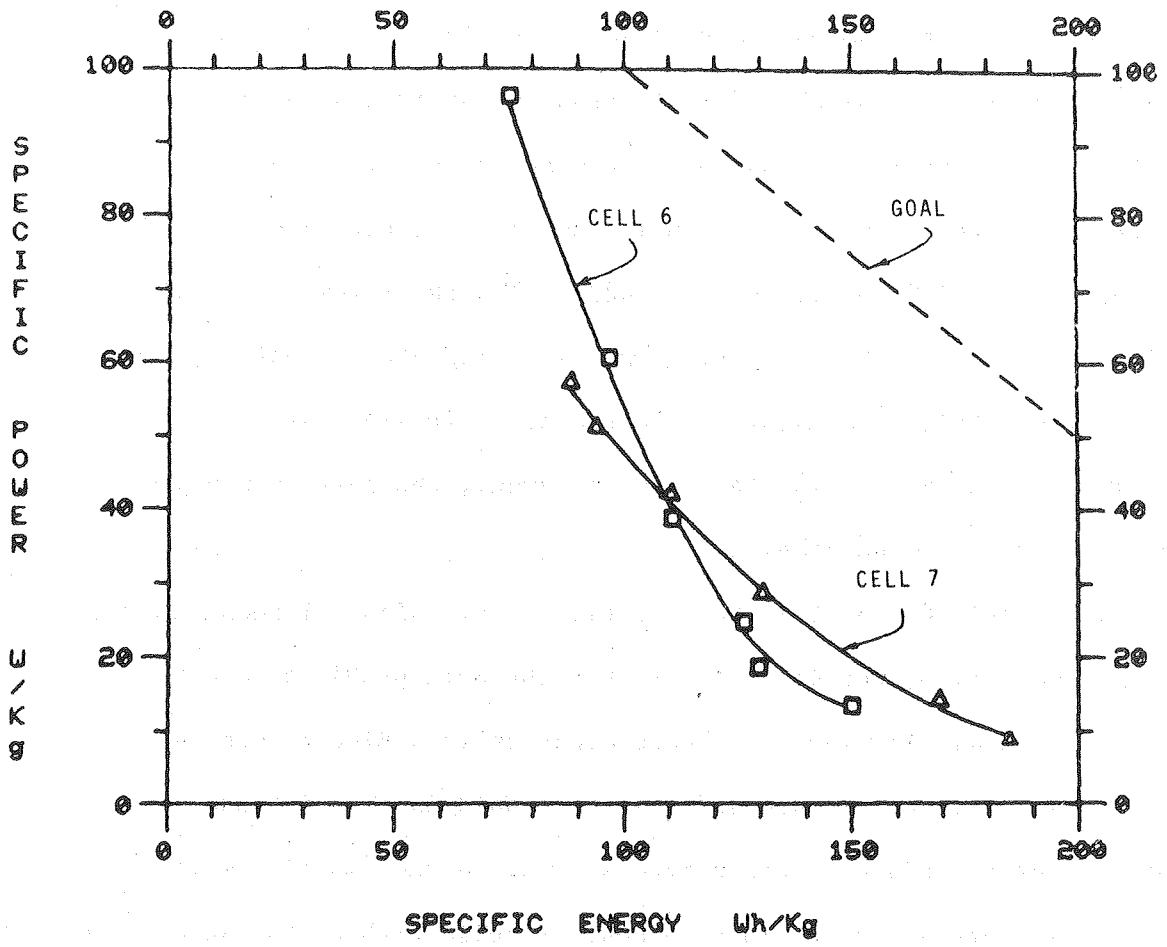

XBL 802-8065

cycles and lifetimes of over 15,000 h can be achieved (see Figure 17). Even though good progress has been made in developing long-lived, high specific energy Li_4Si/FeS_2 cells, there are some significant problems requiring additional effort, as indicated in Table 8.

This cell has somewhat more severe materials problems than the LiAl/FeS cell, because the FeS_2 electrode presents a higher sulfur activity to the current collector, narrowing the selection of current collector materials. Presently, molybdenum is used in conjunction with graphite powder. There is some degree of concern with the formation of slightly-soluble sulfur-containing species which can migrate gradually through the electrolyte toward the negative electrode. A full assessment of this problem has not been completed. In any event, the performance and lifetime data reported are encouraging.

The Li_4Si/FeS_2 cell is in an earlier stage of development than the Na/S or LiAl/FeS cells, but it is clear that the main problems have to do with materials, as is the case for those other cells. Electrochemical kinetics and transport processes are sufficiently rapid in all of these systems that rate processes, properly taken into account in the designs, will not present formidable barriers to the development of cells with performance capabilities appropriate for such applications as vehicle propulsion and off-peak energy storage.

3.3 The Calcium-Silicon/Molten Halide/Iron Disulfide Cell

An interesting variant of the cell just described is obtained by replacing the lithium with calcium.[21,22] The negative electrode becomes a calcium-silicon alloy, which can be operated over the range Ca_2Si to at least $CaSi_2$. The electrolyte must contain calcium ions, of course, and the most effective electrolyte investigated is a mixture of 29% LiCl-20% NaCl-35% $CaCl_2$-16% $BaCl_2$,

TABLE 8

$Li_4Si/LiCl-KCl/FeS_2$

$Li_4Si + FeS_2 \rightarrow 2Li_2S + Fe + Si$

E = 1.8, 1.3 V; 944 Wh/kg Theoretical

Status

Cell Size	70 Ah
Specific Energy	120 Wh/kg @ 30 W/kg
	180 Wh/kg @ 7.5 W/kg
Specific Power	100 W/kg, peak
Cycle Life	700 @ 100% DOD
Lifetime	~15,000 h
Cost	>$1000/kWh

Recent Work

- Bipolar cells
- Li-Si electrodes
- BN felt separators
- 70 Ah cells

Problems

- Materials for FeS_2 current collector
- Leak-free feedthroughs
- High internal resistance
- Low-cost separators needed
- Thermal control

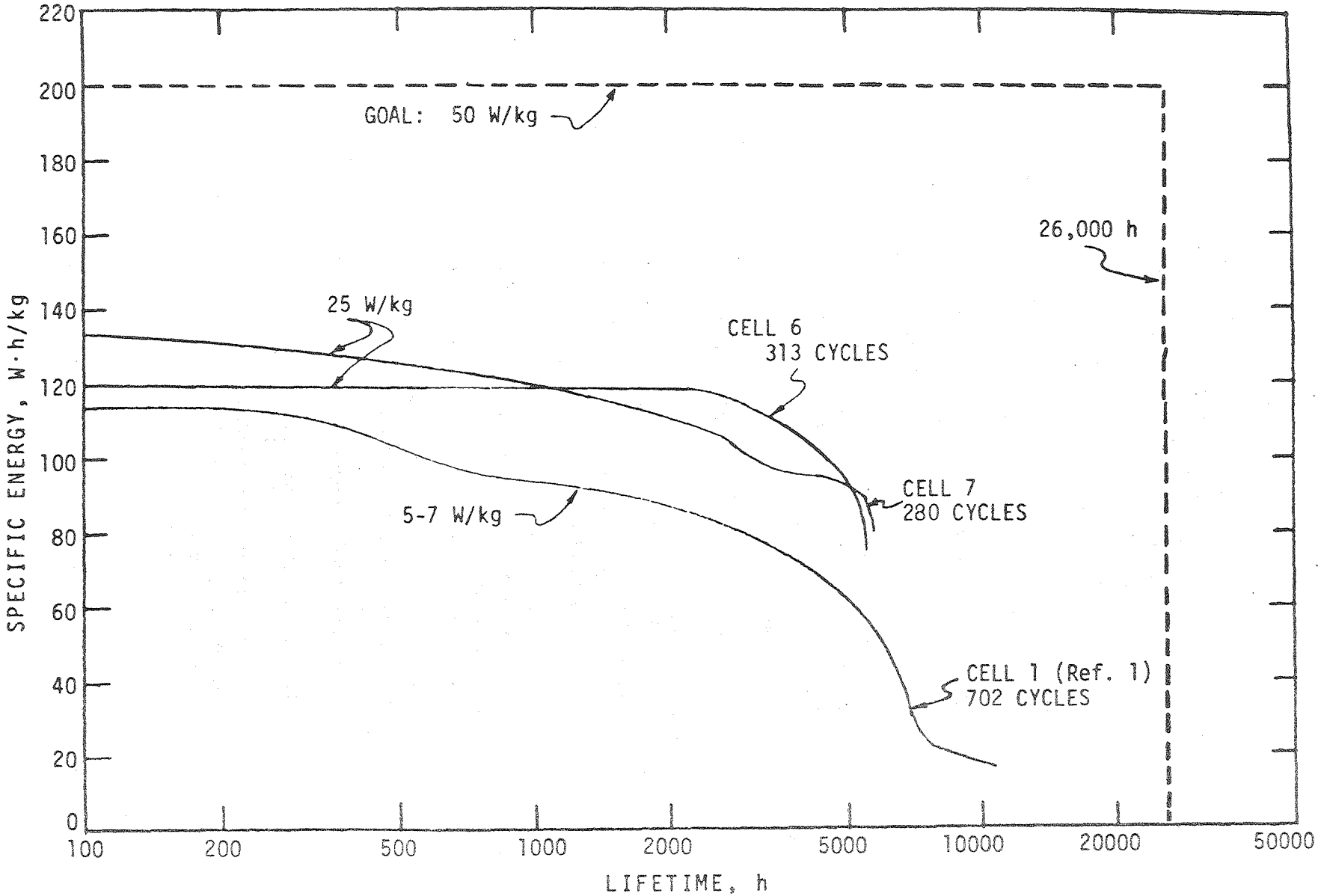
220
200
180
160
140
120
100
80
60
40
20
0
SPECIFIC ENERGY, W·h/kg
GOAL: 50 W/kg
26,000 h
25 W/kg
CELL 6
313 CYCLES
CELL 7
280 CYCLES
5-7 W/kg
CELL 1 (Ref. 1)
702 CYCLES
100
200
500
1000
2000
5000
10000
20000
50000
LIFETIME, h

FIGURE 17

operating at 460°C.

Cells similar in structure to LiAl/FeS and Li_4Si/FeS_2 cells have been operated, but only at low current densities. A cell voltage vs. capacity curve for a 100 Ah cell is shown in Figure 18.[27] The voltage range over which this cell operates is similar to that for Li_4Si/FeS_2, and there is the possible advantage of being able to use the more abundant, lower-cost calcium instead of lithium.

The status of the work on this system is shown in Table 9. Note the low specific power and specific energy. These need improvement in order to make this system sufficiently interesting to work on extending the life to significantly longer values. Successful improvement in the cell performance and lifetime could yield a system of significant practical interest.

4. CONCLUSIONS

The discussion above, regarding various types of high-temperature cells in all stages of research and development, leads to the following conclusions:

- Sodium/sulfur cells with ceramic electrolytes (β- and β"-Al_2O_3) are in the most advanced state of development. Several more multi-kilowatt-hour batteries will be developed and tested, both in Europe, and in the U.S., during the early 1980's. These batteries may find application in vehicle propulsion and stationary energy storage. Thermal cycling remains a problem.
- Variants of the Na/S cell, such as the Na/SCl_3AlCl_4 cell may have advantages in certain applications where lower operating temperatures and higher cell voltages are important. This cell is still in research stages.
- Lithium alloy/iron sulfide cells are making good progress in both lifetime and performance. Full-scale cells are being tested, and

TABLE 9

$Ca_2Si/LiCl-NaCl-CaCl_2-BaCl_2/FeS_2$

$Ca_2Si + FeS_2 \rightarrow 2CaS + Fe + Si$

E = 2.0-1.2 V; ∿750 Wh/kg Theoretical

Status

Specific Energy	40 Wh/kg @ 8 W/kg
Specific Power	<10 W/kg
Cycle Life	60
Cost	too early

Recent Work

$BaCl_2$ added to electrolyte

Larger cells - 100 Ah

Problems

Low specific power

Low current densities

FIGURE 18

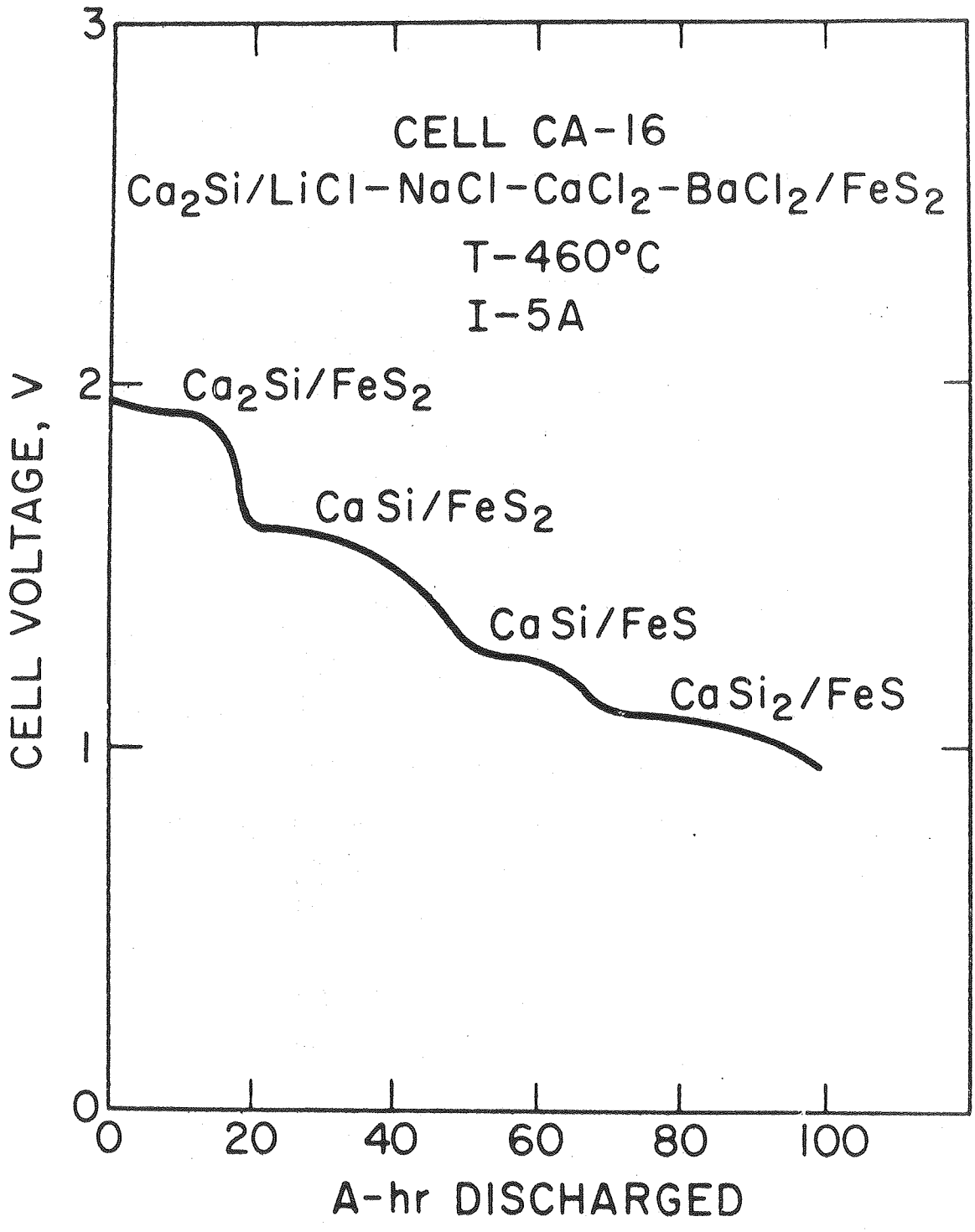

XBL 802-8068

multi-kilowatt hour batteries will be tested in the early 1980's. These systems appear to have promise of being rugged and capable of thermal cycling.

- The calcium-silicon/iron disulfide system may offer a lower-cost option than lithium alloy/iron sulfide cells. This cell is in early stages of R&D.
- Overall, the pace-setting problems for high-temperature batteries are materials and materials-related problems. Major problem areas include sulfur and sulfide-resistant current collectors, corrosion resistant seals and feedthroughs, rugged solid electrolytes, including lithium ion conductors, and alkali metal resistant insulators.

The progress in the research and development of high temperature rechargeable cells and batteries in the last decade has been remarkably good. There are at least a few systems among which to choose, and at last performances and cycle lives greater than those for many, if not all high performance ambient-temperature systems are being realized. These systems have come a long way. Will they be made available commercially in the next decade? The probability is getting higher!

REFERENCES

1. E. J. Cairns and R. K. Steunenberg, High-Temperature Batteries, in: Progress in High Temperature Physics and Chemistry (C. A. Rouse, ed.), Vol. 5, p. 63, Pergamon Press, New York (1973).

2. Y. Y. Yao and J. T. Kummer, J. Inorg. Nucl. Chem. 29, 2453 (1967).

3. J. T. Kummer and N. Weber, A Sodium-sulfur secondary battery, presented at: SAE Automotive Engineering Congress, Detroit, Michigan, Preprint No. 670179 (January 9-13, 1967).

4. N. K. Gupta and R. P. Tischer, J. Electrochem. Soc. 119, 1033 (1972).

5. F. Ludwig, A Review of the Kinetics of the Sulfur Electrode in Molten Polysulfide, in: Proceedings of the Symposium and Workshop on Advanced Battery Research and Design, Argonne National Lab Report No. ANL 76-8 (March 1976).

6. R. W. Minck, The Performance of Shaped Graphite Electrodes in Sodium Sulfur Cells, in: Proceedings of the Symposium and Workshop on Advanced Battery Research and Design, Argonne National Lab Report No. ANL 76-8 (March, 1976).

7. G.E. Review of the Advanced Battery Development Program for Electric

Utility Application (May 16, 1979).

8. W. Fischer, H. B. Gels, F. Gross, K. Liemert, and H. Meinhold, Sodium/Sulfur Batteries for Peak Power Generation, in: Proceedings of the 14th IECEC, p. 710, Amer. Chem. Soc., Washington, D.C. (1979).

9. C. A. Levine, Progress in the Development of the Hollow Fiber Na-S Secondary Cell, in: Proceedings of the 10th IECEC, p. 621, Inst. of Elec. and Electronic Engrs., New York (1975).

10. J. Werth, Alakli Metal-Metal Chloride Battery, U.S. Pat. 3,887,984 (April 15, 1975).

11. J. Werth, Sodium Chloride Battery Development Program for Hood Leveling, Research Report 109-2-1 to Electric Power Research Institute (June, 1975).

12. J. Werth, Sodium Chloroaluminate Battery, in: Proceedings of the Symposium and Workshop on Advanced Battery Research and Design, p. B263, Argonne National Lab Report No. ANL 76-8 (March, 1976).

13. G. Mamantov, Studies of High Energy Cathodes and Anodes for Molten Salt Batteries, Progress Report to U.S. Department of Energy (August, 1978 - July, 1979).

14. E. J. Cairns and H. Shimotake, High-Temperature Batteries, Science 164, 1347 (1969).

15. E. J. Cairns, J. P. Ackerman, P. D. Hunt, and B. S. Tani, The Thermodynamics and Electrochemistry of the Lithium/Sulfur Cell by EMF and Phase Equilibration Methods, presented at The Electrochemical Society Meeting, Cleveland, Ohio, Abstract No. 48 (October, 1971); See also Extended Abstracts, p. 118.

16. E. J. Cairns, H. Shimotake, E. C. Gay, M. L. Kyle and R. K. Steunenberg, Lithium/Sulfur Secondary Cells, presented at the International Society of Electrochemistry Meeting, Stockholm, Sweden (August 28 - September 2, 1972).

17. E. S. Buzzelli, Aluminum Anode Electrical Energy Storage Device, U.S. Patent No. 3,445,288 (May 20, 1969).

18. N. P. Yao, L. A. Heredy and R. C. Saunders, Secondary Lithium/Sulfur Battery, presented at The Electrochemical Society Meeting, Atlantic City, New Jersey (October, 1970).

19. S. Lai and L. McCoy, Lithium-Silicon Electrode, presented at The Electrochemical Society Meeting, Dallas, Texas (October, 1975).

20. R. A. Sharma and R. N. Seefurth, Thermodynamic Properties of the Lithium-Silicon System, J. Electrochem. Soc. 123, 1763 (1976).

21. S. K. Preto and M. F. Roche, Electrochemistry of FeS_2, CoS_2 and NiS_2 Electrodes in Calcium Cells, presented at The Electrochemical Society Meeting, Los Angeles, California (October, 1979); Extended Abstracts 79-2, p. 391 (1979).

22. M. F. Roche, L. E. Ross, C. C. Sy, S. K. Preto, L. G. Bartholme and P. F. Eshman, High-Performance Batteries for Electric-Vehicle Propulsion and Stationary Energy Storage, Progress Report for the Period October 1978-March 1979, in: Argonne National Lab Report ANL 70-39, pp. 94-106 (May, 1979).

23. P. A. Nelson, D. L. Barney, R. K. Steunenberg, A. A. Chilenskas, E. C. Gay, J. E. Battles, F. Hornstra, W. E. Miller, M. F. Roche, H. Shimotake, R. Hudson, R. J. Rubischko and S. Sudar, High Performance Batteries for Electric-Vehicle Propulsion and Stationary Energy Storage, Progress Report for the Period October 1977-September 1978, in: Argonne National Lab Report ANL 78-94 (November, 1978).

24. H. Shimotake, W. J. Walsh, E. S. Carr and L. G. Bartholme, Development of Uncharged Li-Al/FeS_x Cells, in: Proceedings of the 11th IECEC, Vol. 1, p. 473, American Institute of Chemical Engineers, New York (1976).

25. M. L. Saboungi, C. Bale, P. L. Lin, M. Blander and A. Pelton, Calculations of Phase Equilibria for Molten Salt Batteries and Fuel Cells from Fundamental Solution Theories, presented at The Electrochemical Society Meeting, Los Angeles, California, Abstract No. 157 (October, 1979); See Extended Abstracts, 79-2, 405 (1979).

26. K. M. Myles, F. C. Mrazek, J. A. Smaga and J. L. Settle, Materials Development in the Lithium-Aluminum/Iron Sulfide Battery Program at Argonne National Laboratory, in: Proceedings of the Symposium and Workshop on Advanced Battery Research and Design, March 22-24, 1976, Argonne National Lab Report ANL-76-8, p. B-69 (1976).

27. Argonne National Laboratory, Annual DOE Review of the Lithium/Metal Sulfide Battery Program (June, 1979).

28. E. J. Zeitner and J. S. Dunning, High Performance Lithium/Iron Disulfide Cells, Proceedings of the 13th IECEC, Soc. Automotive Engrs., Warrendale, Pennsylvania, p. 697 (1978).

FIGURE CAPTIONS

Figure 1 Theoretical specific energy (W-h/kg) for various electrochemical couples plotted against the sum of the molecular weights of the reactants times the number of moles of each involved in the balanced cell reaction. The straight lines are iso-EMF lines. A good approximation to practical specific energies is obtained by multiplying the values in the figure by 0.2-0.25 for couples with solid reactants, and 0.15-0.2 if gaseous reactants are involved.

Figure 2 Cross section of a sodium/beta-alumina/sulfur cell, using the sodium-core design.

Figure 3 The sodium-sulfur phase diagram, after Gupta and Tischer.[4]

Figure 4 The reversible emf of the sodium/sulfur cell as a function of the sulfur electrode composition.[1]

Figure 5 Exploded view of a 168 Ah sodium/sulfur cell of the sodium-core design.[7]

Figure 6 Voltage-current curve of a 96-cell, 10 kWh sodium/sulfur battery.[8] The cells were connected as four parallel strings of 24 cells each, with cross-connections between strings every 8 cells. Each cell was nominally 48 Ah. The battery yielded 177 Ah, with an energy efficiency of 61%.

Figure 7 Schematic cross section of the hollow glass fiber sodium/sulfur cell.[9]

Figure 8 Voltage-capacity curve for a LiAl/FeS cell.[24]

Figure 9 Isothermal section of the Li-Fe-S phase diagram at 450°C.[22]

Figure 10 The lithium-aluminum phase diagram.[26]